NASA Technical Paper 1419

Low-Speed Wind-Tunnel Parametric Investigation of Flight Spoilers as Trailing-Vortex-Alleviation Devices on a Transport Aircraft Model

Delwin R. Croom

APRIL 1979

NASA

NASA Technical Paper 1419

Low-Speed Wind-Tunnel Parametric Investigation of Flight Spoilers as Trailing-Vortex-Alleviation Devices on a Transport Aircraft Model

Delwin R. Croom
Langley Research Center
Hampton, Virginia

National Aeronautics
and Space Administration

**Scientific and Technical
Information Office**

1979

SUMMARY

An investigation was made in the Langley V/STOL tunnel to determine, by the trailing-wing sensor technique, the effectiveness of 11 combinations of the existing flight-spoiler segments on a jumbo-jet transport aircraft model when they were deflected as trailing-vortex-alleviation devices. All 11 of the flight-spoiler configurations investigated were effective in reducing the induced rolling moment on the trailing model by as much as 18 to 67 percent at a distance of 7.8 transport wing spans behind the transport aircraft model. The present investigation is an extension of earlier wind-tunnel and flight tests which showed that the existing flight spoilers on the jumbo-jet aircraft can be used as effective trailing-vortex-alleviation devices.

Essentially all of the reduction in induced rolling moment on the trailing-wing model was realized at a spoiler deflection of 45° for single-spoiler configurations, 30° for two-spoiler configurations, and 15° for both the three- and four-spoiler configurations.

Of the 11 flight-spoiler configurations investigated, the most promising configuration for trailing-vortex abatement on the jumbo-jet aircraft appears to be the three inboard flight spoilers deflected 15°. This configuration reduced induced rolling moment on the trailing-wing model by 65 percent and increased drag coefficient on the transport aircraft model by about 0.012 at a trim lift coefficient of 1.2.

INTRODUCTION

The strong vortex wakes generated by large transport aircraft are a potential hazard to smaller aircraft. The National Aeronautics and Space Administration is involved in a program of model tests, flight tests, and theoretical studies to investigate aerodynamic means of reducing this hazard (ref. 1).

Results of recent investigations have indicated that the trailing vortex behind an unswept-wing model (ref. 2) or a swept-wing transport model (ref. 3) can be attenuated by a forward-mounted spoiler. It was also determined by model tests (refs. 4, 5, and 6) and verified in full-scale flight tests that there are several combinations of the existing flight spoilers on both the jumbo-jet transport aircraft (ref. 7) and a medium-range wide-body tri-jet transport aircraft (ref. 8) that are effective as trailing-vortex-alleviation devices. The approach used in references 2 to 6 to evaluate the effectiveness of vortex-alleviation devices was to simulate an airplane flying in the trailing vortices of another larger airplane and to make direct measurements of rolling moments induced on the trailing model by the vortices generated by the forward model. The technique used in the full-scale flight tests (refs. 7 and 8) was to penetrate the trailing-vortex wake behind a Boeing 747 aircraft (ref. 7) and behind a Lockheed L-1011 aircraft (ref. 8) with a Cessna T-37 aircraft and to evaluate

the roll response and roll attitude of the Cessna T-37 aircraft as an index of the severity of the trailing-vortex encounter.

Since there were a limited number of flight-spoiler combinations investigated in reference 4, the purpose of the present investigation is to determine whether other flight-spoiler combinations on the jumbo-jet transport aircraft model would give greater trailing-vortex alleviation than those reported in reference 4. The direct-measurement technique described in references 2 to 6 was used with the trailing-wing model at 7.8 transport wing spans behind the transport aircraft model. For the full-scale transport airplane, this would represent a downstream distance of 0.25 nautical mile.

The use of commercial airplane designations in this report does not constitute an official endorsement of such products or manufacturers, either expressed or implied, by the National Aeronautics and Space Administration.

SYMBOLS

All data are referenced to the wind axes. The pitching-moment coefficients are referenced to the quarter-chord of the wing mean aerodynamic chord.

b wing span, m

C_D drag coefficient, $\dfrac{\text{Drag}}{qS_W}$

C_L lift coefficient, $\dfrac{\text{Lift}}{qS_W}$

$C_{l,TW}$ trailing-wing rolling-moment coefficient, $\dfrac{\text{Trailing-wing rolling moment}}{qS_{TW}b_{TW}}$

C_m pitching-moment coefficient, $\dfrac{\text{Pitching moment}}{qS_W\bar{c}_W}$

c wing chord, m

$\bar{c}$ wing mean aerodynamic chord, m

i_t horizontal-tail incidence, referred to fuselage reference line (positive direction, trailing edge down), deg

q free-stream dynamic pressure, Pa

S wing area, m^2

X',Y',Z' system of axes originating at left wing tip of transport aircraft model (see fig. 1)

x',y',z' longitudinal, lateral, and vertical dimensions measured from trailing edge of left wing tip of transport aircraft model, m

α angle of attack of fuselage reference line (wing incidence is 2° relative to fuselage reference line), deg

Subscripts:

max maximum

TW trailing-wing model

W transport aircraft model

MODEL AND APPARATUS

A three-view sketch and the principal geometric characteristics of the 0.03-scale model of the jumbo-jet transport aircraft are shown in figure 1. Figure 2 is a photograph of the transport aircraft model sting mounted in the Langley V/STOL tunnel. The fuselage, empennage, trailing-edge flaps, and leading-edge devices of this model were the same as those used in references 3 and 4. The wing had flight spoilers typical of this type of aircraft. Figure 3 is a sketch showing the location and numbering of the flight-spoiler segments on the transport aircraft model. Photographs of 9 of the 11 flight-spoiler configurations investigated are presented in figure 4. (Not shown are two single-spoiler configurations, segment 2 and segment 3.)

A photograph and dimensions of the unswept trailing-wing model installed on the traverse mechanism are presented in figure 5. The trailing model has a span and aspect ratio typical of small-size transport aircraft.

The test section of the Langley V/STOL tunnel has a height of 4.42 m, a width of 6.63 m, and a length of 14.24 m. The transport aircraft model was sting mounted near the forward end of the tunnel test section on a six-component strain-gage balance system which measured the forces and moments. The angle of attack was determined from an accelerometer mounted in the fuselage. The trailing model was mounted on a single-component strain-gage roll balance, which was attached to a traverse mechanism capable of moving the model both laterally and vertically. (See fig. 5.) The lateral and vertical positions of the trailing model were measured by outputs from digital encoders. This entire traverse mechanism could be mounted to the tunnel floor at various tunnel longitudinal positions downstream of the transport aircraft model.

TESTS AND CORRECTIONS

Transport Aircraft Model

All tests were made at a free-stream dynamic pressure in the tunnel test section of 430.9 Pa which corresponds to a velocity of 27.4 m/sec. The Reynolds number for the tests was approximately 4.7×10^5 based on the wing mean aerodynamic chord. Transition strips approximately 0.30 cm wide of No. 60 abrasive grit were placed 2.54 cm back from the leading edge of the wing, whereas natural transition was used elsewhere. The basic longitudinal aerodynamic characteristics were obtained through an angle-of-attack range of approximately -4° to 24°. All tests were made with leading-edge devices extended, landing gear down, and landing flaps deflected 30°.

Blockage corrections were applied to the data by the method of reference 9. Jet-boundary corrections to the angle of attack and the drag were applied in accordance with reference 10.

Trailing-Wing Model

The trailing-wing model and its associated roll-balance system were used as a sensor to measure the induced rolling moment caused by the vortex flow downstream of the transport aircraft model. No transition grit was applied to the trailing model. The trailing model was positioned near the aft end of the tunnel test section (7.8 transport wing spans behind the transport aircraft model), and the traverse mechanism was positioned laterally and vertically so that the trailing vortex was near the center of the mechanism. The trailing vortex was probed with the trailing model. A large number of trailing-wing rolling-moment data points (usually from 50 to 100) were obtained from the lateral traverses at several vertical locations to ensure good definition of the vortex wake so that the maximum trailing-wing rolling-moment coefficient could be determined. In addition, certain test conditions were repeated at selected intervals during the test period and the data were found to be repeatable. All trailing-wing rolling-moment data were obtained with the transport aircraft model at a trimmed lift coefficient of 1.2 ($C_{L,trim} = 1.2$).

RESULTS AND DISCUSSION

Transport Aircraft Model

The longitudinal aerodynamic characteristics of the transport aircraft model with 11 different flight-spoiler configurations deflected symmetrically through a range of 0° to 45° are presented in figures 6 to 16. Table I lists the 11 spoiler configurations. These data (figs. 6 to 16) were obtained with the horizontal tail set at 0° ($i_t = 0^\circ$). Below the stall, there is essentially a linear increase in drag with spoiler deflection for all these configurations. The increase in drag coefficient ranges from about 0.002 to about 0.06. Also for all of these configurations, about 50 percent of the lift loss at a given angle

of attack occurs at a spoiler deflection of about 15°. Generally, when the spoilers are deflected, the linear range of the pitching-moment coefficient is extended to a higher angle of attack.

The data for the single-spoiler configurations (figs. 6, 7, 8, and 9) indicate that, at the maximum spoiler deflection angle of 45°, a nominal lift coefficient of 1.2 can be maintained with an increase in angle of attack of less than 1.5°. At the maximum spoiler deflection angle of 45°, the increase in angle of attack to maintain a nominal lift coefficient of 1.2 was about 2.5° for the two-spoiler configurations (figs. 10, 13, 15, and 16), about 3.5° for the three-spoiler configurations (figs. 11 and 14), and about 4° for the four-spoiler configuration (fig. 12). At a lift coefficient of 1.2, the maximum increase in drag associated with the spoiler configurations deflected 45° was about 0.03 for the single-spoiler configurations, about 0.04 for the two-spoiler configurations, about 0.05 for the three-spoiler configurations, and about 0.06 for the four-spoiler configurations.

Trailing-Wing Model

The maximum rolling-moment coefficient measured by the trailing model and the position of this model relative to the left wing tip of the transport aircraft model are presented in figures 17 to 20 as a function of flight spoiler deflection for the various combinations of flight-spoiler segments investigated. Eleven flight spoiler combinations were investigated and all were effective in reducing the induced rolling moment on the trailing-wing model by as much as 18 to 67 percent. These data were obtained with the trailing-wing model positioned 7.8 transport wing spans behind the transport aircraft model at $C_{L,trim} = 1.2$. The horizontal-tail incidence angle (i_t), required to trim the transport aircraft model at a lift coefficient of 1.2 ($C_{L,trim} = 1.2$) and the associated measured drag coefficient are listed in table II for the various combinations of flight spoilers.

For all of the spoiler configurations investigated, the maximum rolling moment on the trailing-wing model was obtained with the trailing-wing model located inboard of and below the transport aircraft model wing tip (figs. 17 to 20).

It can be seen in figure 17 that, for any of the single-spoiler configurations, the induced rolling moment $(C_{l,TW})_{max}$ on the trailing model decreased with an increase in spoiler deflection angle throughout the spoiler deflection range of 0° to 45°. The greatest reduction in $(C_{l,TW})_{max}$ from a single-spoiler configuration (about 48 percent) was realized with spoiler segment 3 at a deflection angle of 45°. For all of the two-spoiler configurations (fig. 20), essentially all of the reduction in $(C_{l,TW})_{max}$ was realized at a spoiler deflection angle of about 30° with the largest reduction in $(C_{l,TW})_{max}$ (about 67 percent) being realized for spoiler segments 2 and 4 at a deflection angle of 30°. For both the three- and four-spoiler configurations (figs. 18 and 19), the reduction in $(C_{l,TW})_{max}$ was greater when the spoilers were deflected only 15°. For the three-spoiler configurations, the largest reduction in $(C_{l,TW})_{max}$ (about 65 percent) was realized with spoiler segments 2, 3, and 4 at a deflec-

tion angle of 15°. For the four-spoiler configuration, the largest reduction in $(C_{l,TW})_{max}$ (about 53 percent) was realized with the spoiler segments at a deflection angle of 15°. Some of these spoiler combinations at their higher deflection angles could impose unacceptable performance penalties on the airplane. These penalties include such things as excessive body attitude at landing, due to the increase in angle of attack required to maintain a given lift coefficient, or an increase in noise, due to the increase in engine thrust required to overcome the drag increase. However, these results show that three combinations of spoiler segments and deflections offer significant trailing-vortex abatement without obviously unacceptable performance penalties.

The flight-spoiler configuration of segments 1 and 2, at a deflection angle of 30°, which gave a reduction in $(C_{l,TW})_{max}$ of about 46 percent, was shown to be very effective in attenuating the trailing vortex in full-scale flight tests of the jumbo-jet transport aircraft (ref. 7). Therefore, it appears that the spoiler configurations of segments 2 and 4 at a deflection angle of 30° (which reduces $(C_{l,TW})_{max}$ by about 67 percent) or segments 2, 3, and 4 at a deflection angle of 15° (which reduces $(C_{l,TW})_{max}$ by about 65 percent) should be even more effective in attenuating the trailing vortex behind the jumbo-jet transport. From an aircraft operational standpoint, the spoiler configuration of segments 2, 3, and 4 at a deflection angle of 15° (which increases drag by about 0.012 at $C_{L,trim} = 1.2$) would be more attractive for vortex abatement than either of the spoiler configurations of segments 2 and 4 at a deflection angle of 30° (which increases drag by about 0.026 at $C_{L,trim} = 1.2$) or segments 1 and 2 at a deflection angle of 30° (which increases drag by about 0.026 at $C_{L,trim} = 1.2$).

SUMMARY OF RESULTS

Results have been presented of an investigation in the Langley V/STOL tunnel to determine, by the trailing-wing sensor technique, the trailing-vortex-alleviation effectiveness of various combinations of spoiler segments on a jumbo-jet transport aircraft model when the spoilers are deflected as trailing-vortex-alleviation devices.

Eleven flight spoiler combinations were investigated and all were found to be effective in reducing the induced rolling moment on the trailing-wing model by as much as 18 to 67 percent. The largest reductions realized were 48 percent for the single-spoiler configurations, 67 percent for the two-spoiler configurations, 65 percent for the three-spoiler configurations, and 53 percent for the four-spoiler configuration. The associated increase in drag coefficient for these spoiler configurations ranged from about 0.002 to about 0.06.

Results from tests of the 11 flight-spoiler configurations made over a deflection range of 0° to 45° indicate that essentially all of the reduction in induced rolling moment on the trailing-wing model was realized at a spoiler deflection of 45° for single-spoiler configurations, 30° for two-spoiler configurations, and 15° for both the three- and four-spoiler configurations.

Of the 11 flight-spoiler configurations investigated, the most promising configuration for trailing-vortex abatement on the jumbo-jet aircraft appears to be the three inboard flight spoilers deflected 15°. This configuration reduced induced rolling moment on the trailing-wing model by 65 percent and increased drag coefficient on the transport aircraft model by about 0.012 at a trim lift coefficient of 1.2.

Langley Research Center
National Aeronautics and Space Administration
Hampton, VA 23665
March 5, 1979

REFERENCES

1. Wake Vortex Minimization. NASA SP-409, 1977.

2. Croom, Delwin R.: Low-Speed Wind-Tunnel Investigation of Forward-Located Spoilers and Trailing Splines as Trailing-Vortex Hazard-Alleviation Devices on an Aspect-Ratio-8 Wing Model. NASA TM X-3166, 1975.

3. Croom, Delwin R.; and Dunham, R. Earl, Jr.: Low-Speed Wind-Tunnel Investigation of Span Load Alteration, Forward-Located Spoilers, and Splines as Trailing-Vortex-Hazard Alleviation Devices on a Transport Aircraft Model. NASA TN D-8133, 1975.

4. Croom, Delwin R.: Low-Speed Wind-Tunnel Investigation of Various Segments of Flight Spoilers as Trailing-Vortex-Alleviation Devices on a Transport Aircraft Model. NASA TN D-8162, 1976.

5. Croom, Delwin R.; Vogler, Raymond D.; and Williams, Geoffrey M.: Low-Speed Wind-Tunnel Investigation of Flight Spoilers as Trailing-Vortex-Alleviation Devices on a Medium-Range Wide-Body Tri-Jet Airplane Model. NASA TN D-8360, 1976.

6. Croom, Delwin R.; Vogler, Raymond D.; and Thelander, John A.: Low-Speed Wind-Tunnel Investigation of Flight Spoilers as Trailing-Vortex-Alleviation Devices on an Extended-Range Wide-Body Tri-Jet Airplane Model. NASA TN D-8373, 1976.

7. Barber, Marvin R.; Hastings, Earl C., Jr.; Champine, Robert A.; and Tymczyszyn, Joseph J.: Vortex Attenuation Flight Experiments. Wake Vortex Minimization, NASA SP-409, 1977, pp. 369-403.

8. Industry Observer. Aviat. Week & Space Technol., vol. 107, no. 24, Dec. 12, 1977, p. 11.

9. Herriot, John G.: Blockage Corrections for Three-Dimensional-Flow Closed-Throat Wind Tunnels, With Consideration of the Effect of Compressibility. NACA Rep. 995, 1950. (Supersedes NACA RM A7B28.)

10. Gillis, Clarence L.; Polhamus, Edward C.; and Gray, Joseph L., Jr.: Charts for Determining Jet-Boundary Corrections for Complete Models in 7- by 10-Foot Closed Rectangular Wind Tunnels. NACA WR L-123, 1945. (Formerly NACA ARR L5G31.)

TABLE I.- FLIGHT-SPOILER-SEGMENT COMBINATIONS INVESTIGATED

Figure	Spoiler segments								Spoiler deflection, deg				
	Left wing				Right wing								
	1	2	3	4	4	3	2	1	0	7.5	15	30	45
6	X							X	X		X	X	X
7		X					X		X		X	X	X
8			X			X			X		X	X	X
9				X	X				X		X	X	X
10	X	X					X	X	X		X	X	X
11	X	X	X			X	X	X	X	X	X	X	X
12	X	X	X	X	X	X	X	X	X	X	X	X	X
13			X	X	X	X			X		X	X	X
14		X	X	X	X	X	X		X	X	X	X	X
15	X		X			X		X	X		X	X	X
16		X		X	X		X		X		X	X	X

TABLE II.- HORIZONTAL-TAIL INCIDENCE AND DRAG COEFFICIENT FOR FLIGHT-SPOILER-SEGMENT COMBINATIONS

INVESTIGATED AT $C_{L,trim} = 1.2$

Spoiler segments								Spoiler deflection, deg									
Left wing				Right wing				0		7.5		15		30		45	
1	2	3	4	4	3	2	1	$i_{t,trim}$, deg	$C_{D,trim}$	$i_{t,trim}$, deg	$C_{D,trim}$	$i_{t,trim}$, deg	$C_{D,trim}$	$i_{t,trim}$, deg	$C_{D,trim}$	$i_{t,trim}$, deg	$C_{D,trim}$
X							X	-2.0	0.2184			-1.5	0.2261	-1.0	0.2323	-1.0	0.2355
	X					X						-1.0	.2217	-.9	.2308	0	.2454
		X			X							-.9	.2206	-.5	.2288	-.9	.2407
			X	X								----	.2215	-1.0	.2291	-1.5	.2395
X	X					X	X					-.5	.2290	.2	.2380	1.0	.2515
X	X	X			X	X	X			-1.0	0.2208	-.5	.2330	1.0	.2480	2.0	.2658
X	X	X	X	X	X	X	X			-1.0	.2256	0	.2373	1.5	.2610	2.0	.2772
		X	X	X	X							-1.0	.2298	-.5	.2390	0	.2552
	X	X	X	X	X	X				-.8	.2244	-.2	.2307	1.0	.2525	1.0	.2740
X		X			X		X					-.5	.2283	.2	.2403	.8	.2566
	X		X	X		X		↓	↓			-1.0	.2330	0	.2444	0	.2477

Wing

Span, m	1.79
Mean aerodynamic chord, m	0.25
Root chord, m	0.497
Tip chord, m	0.121
Sweepback at quarter chord, deg	37.5
Area, m^2	0.460
Aspect ratio	6.96

Fuselage

Length, m	2.06

Horizontal tail

Span, m	0.664
Area, m^2	0.123
Aspect ratio	3.6

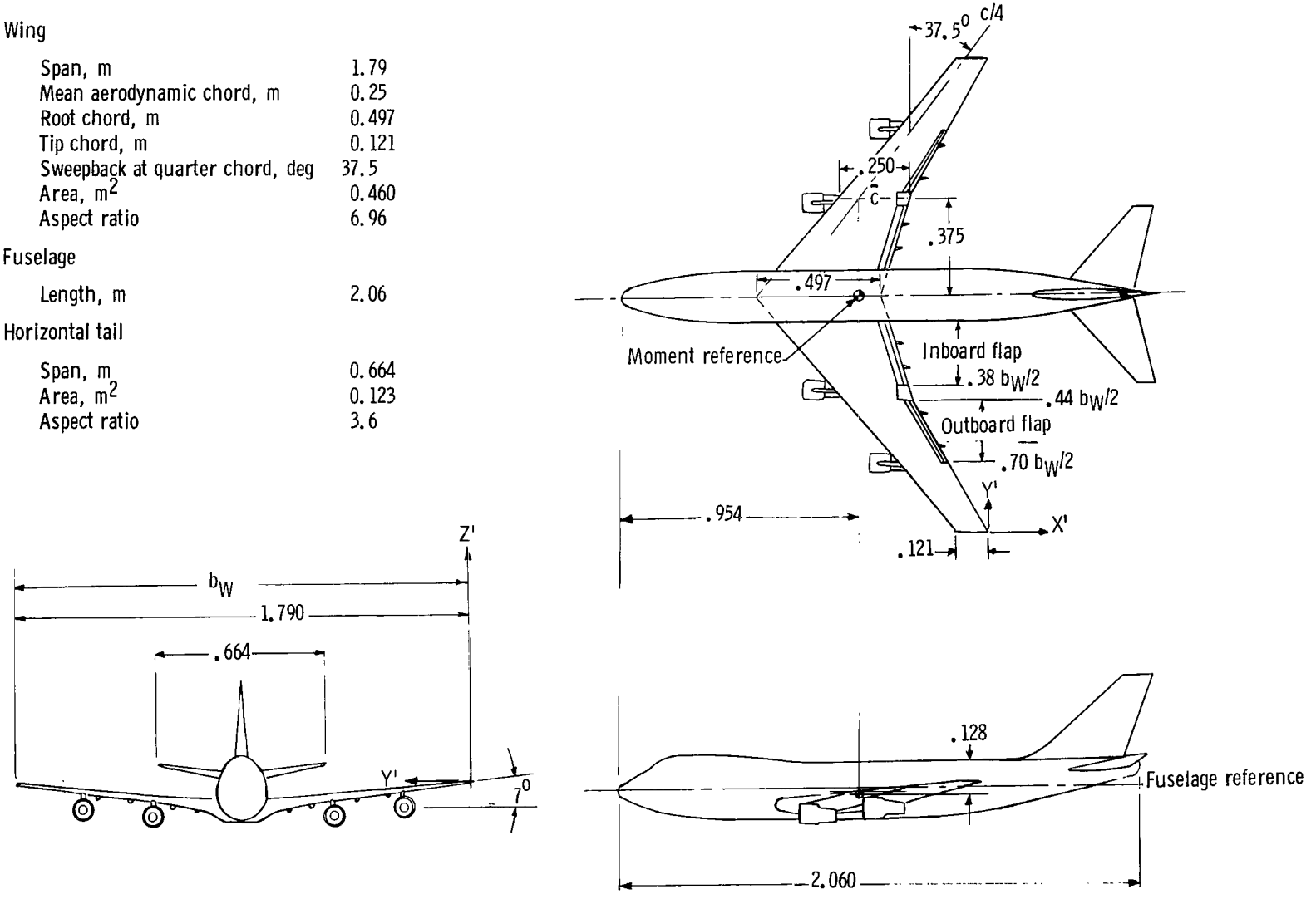

Figure 1.- Three-view sketch of transport aircraft model with flaps retracted. Linear dimensions are in meters.

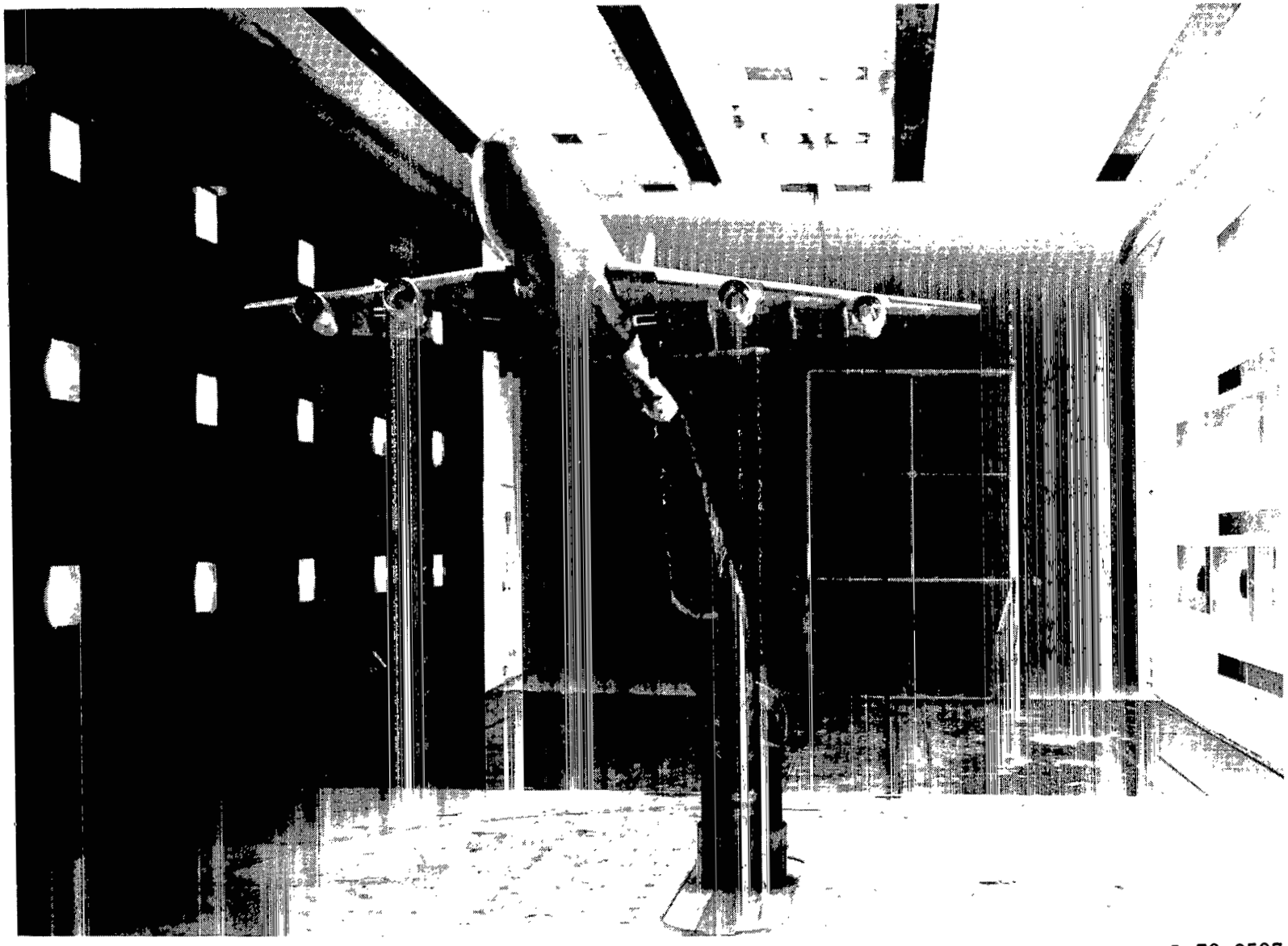

L-78-3587

Figure 2.- Transport aircraft model in the Langley V/STOL tunnel.

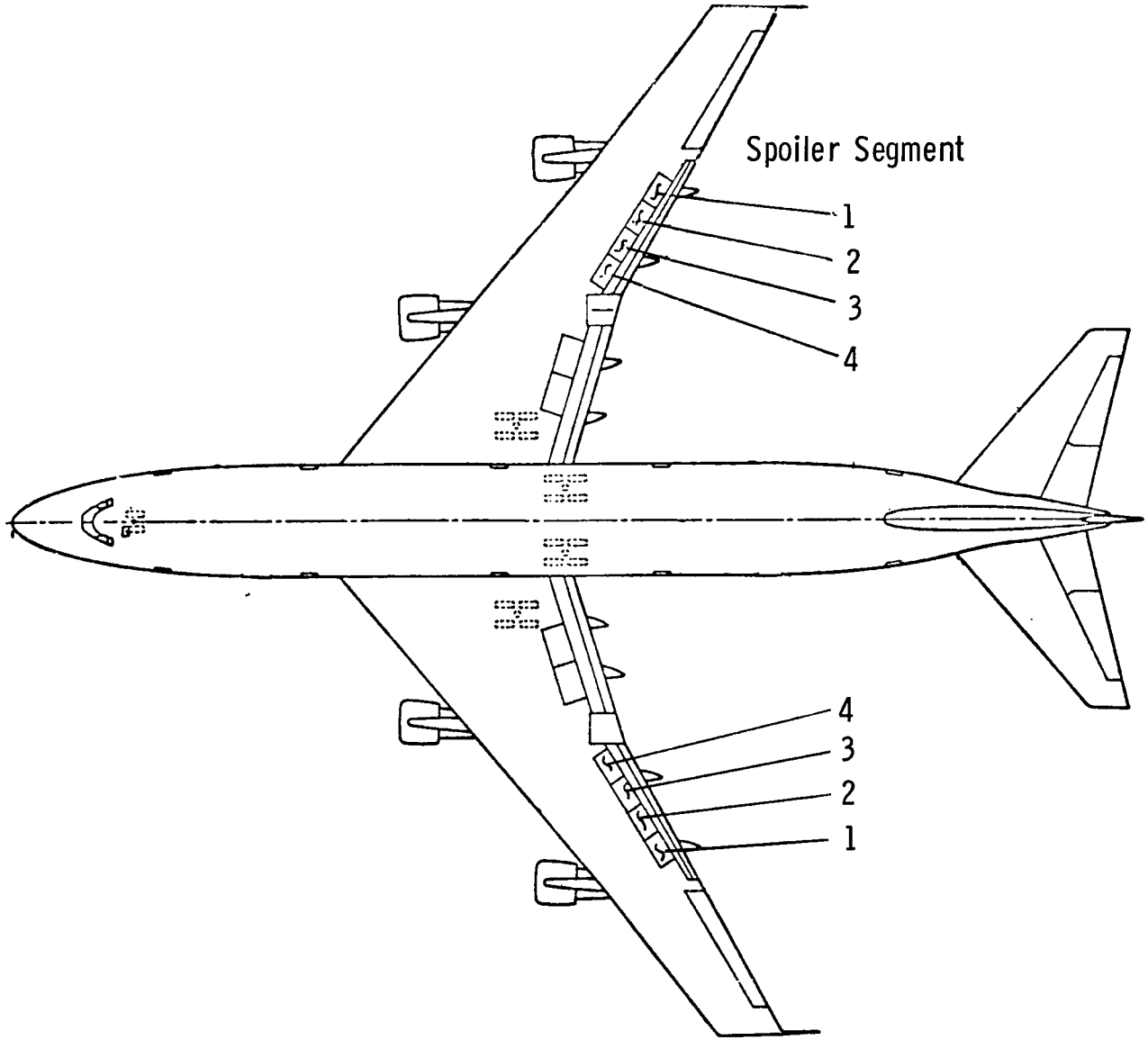

Figure 3.- Sketch of flight-spoiler segments on transport aircraft model.

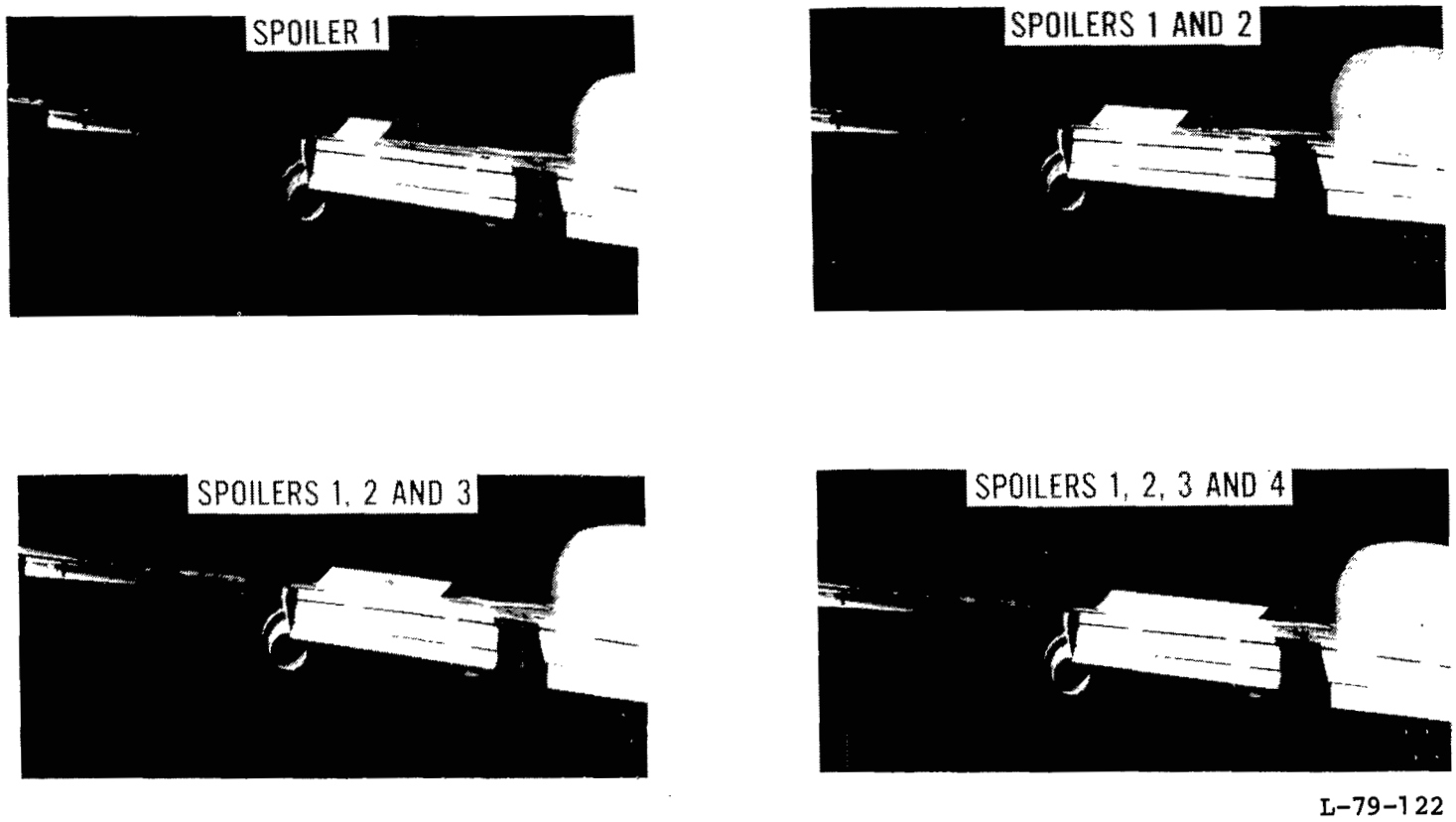

(a) Spoiler segments 1; 1 and 2; 1, 2, and 3; and 1, 2, 3, and 4 deflected 45°.

Figure 4.- Flight-spoiler configurations on transport aircraft model.

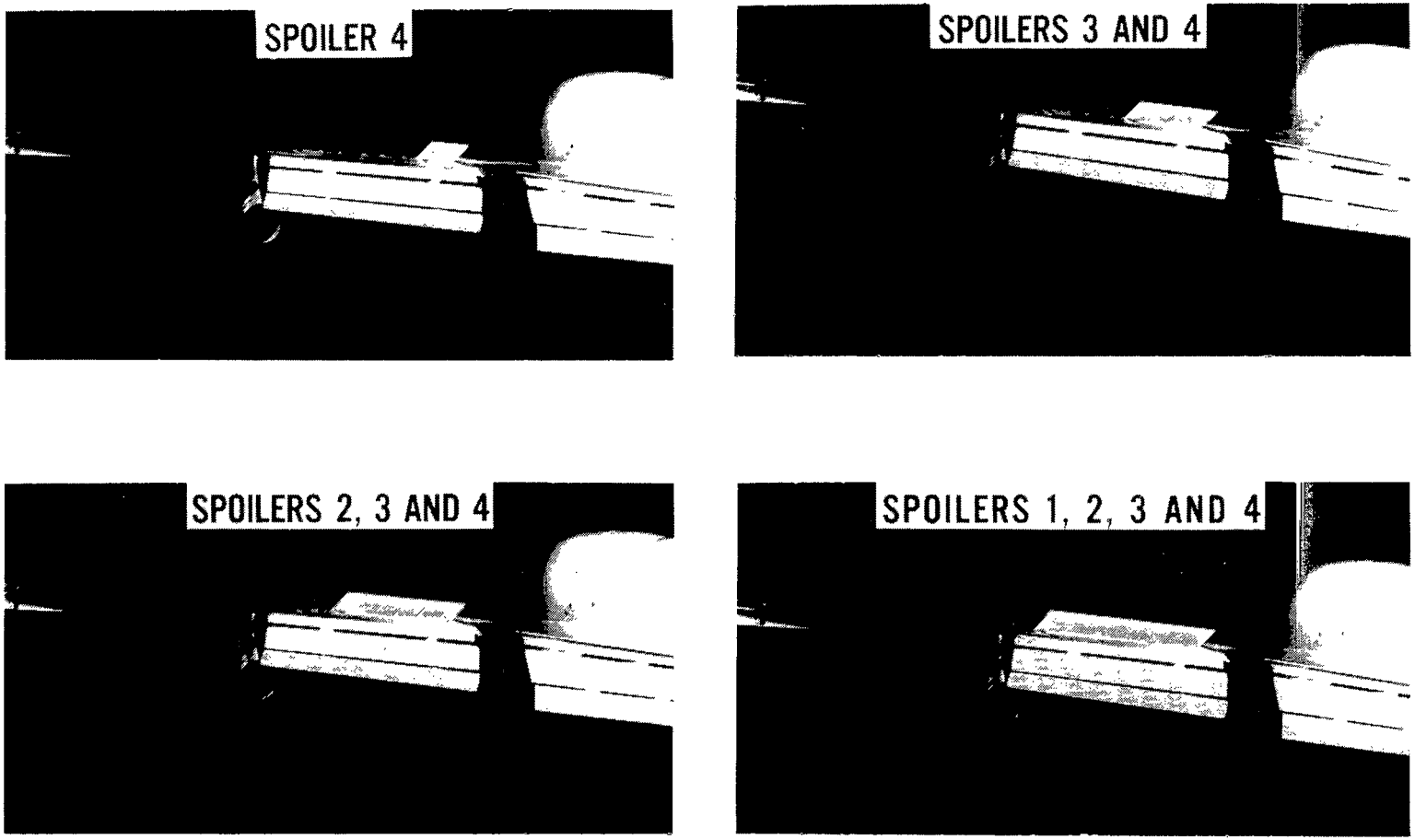

L-79-123

(b) Spoiler segments 4; 3 and 4; 2, 3, and 4; and 1, 2, 3, and 4 deflected 45°.

Figure 4.- Continued.

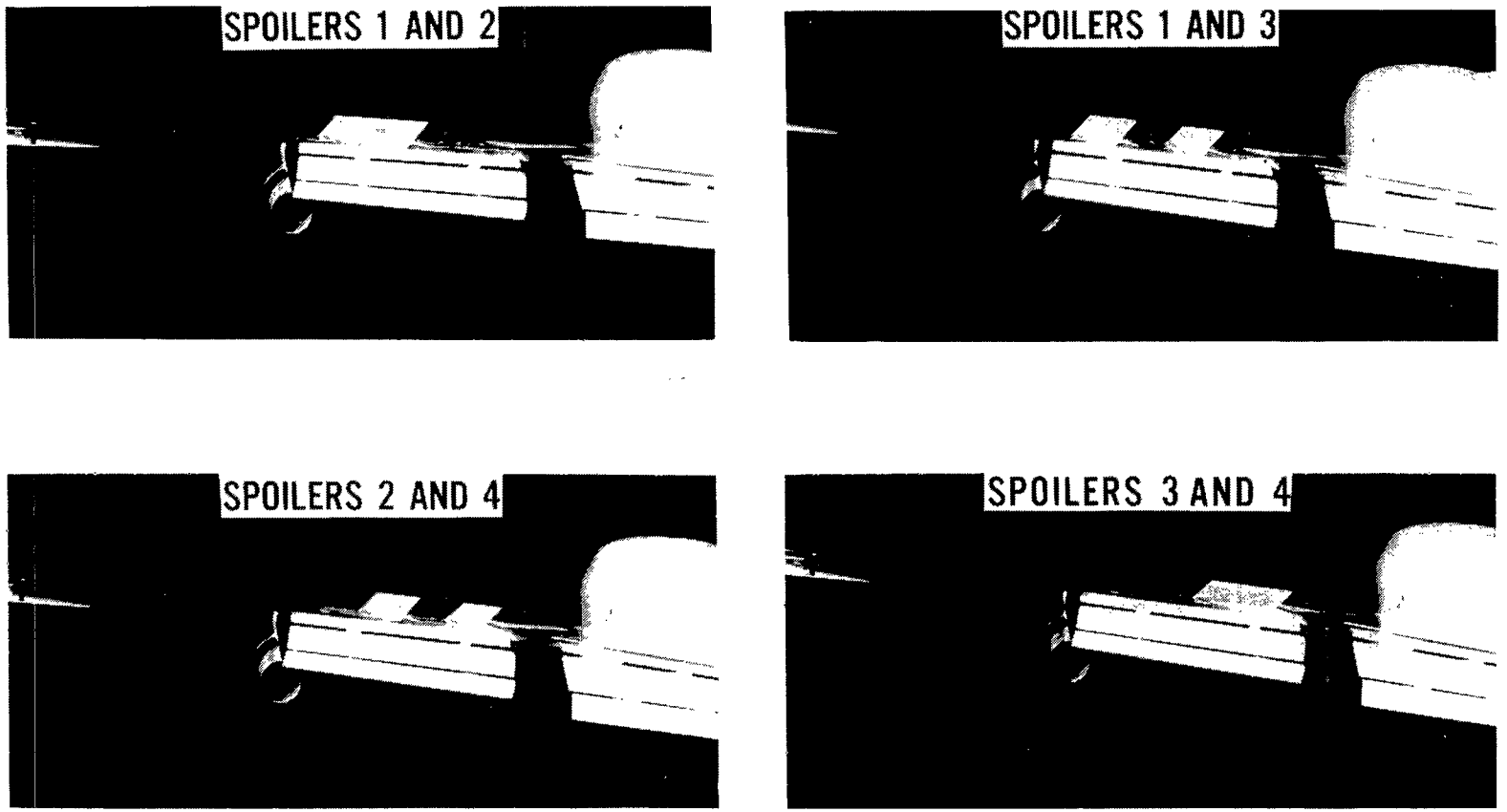

L-79-124

(c) Spoiler segments 1 and 2; 1 and 3; 2 and 4; and 3 and 4 deflected 45°.

Figure 4.- Concluded.

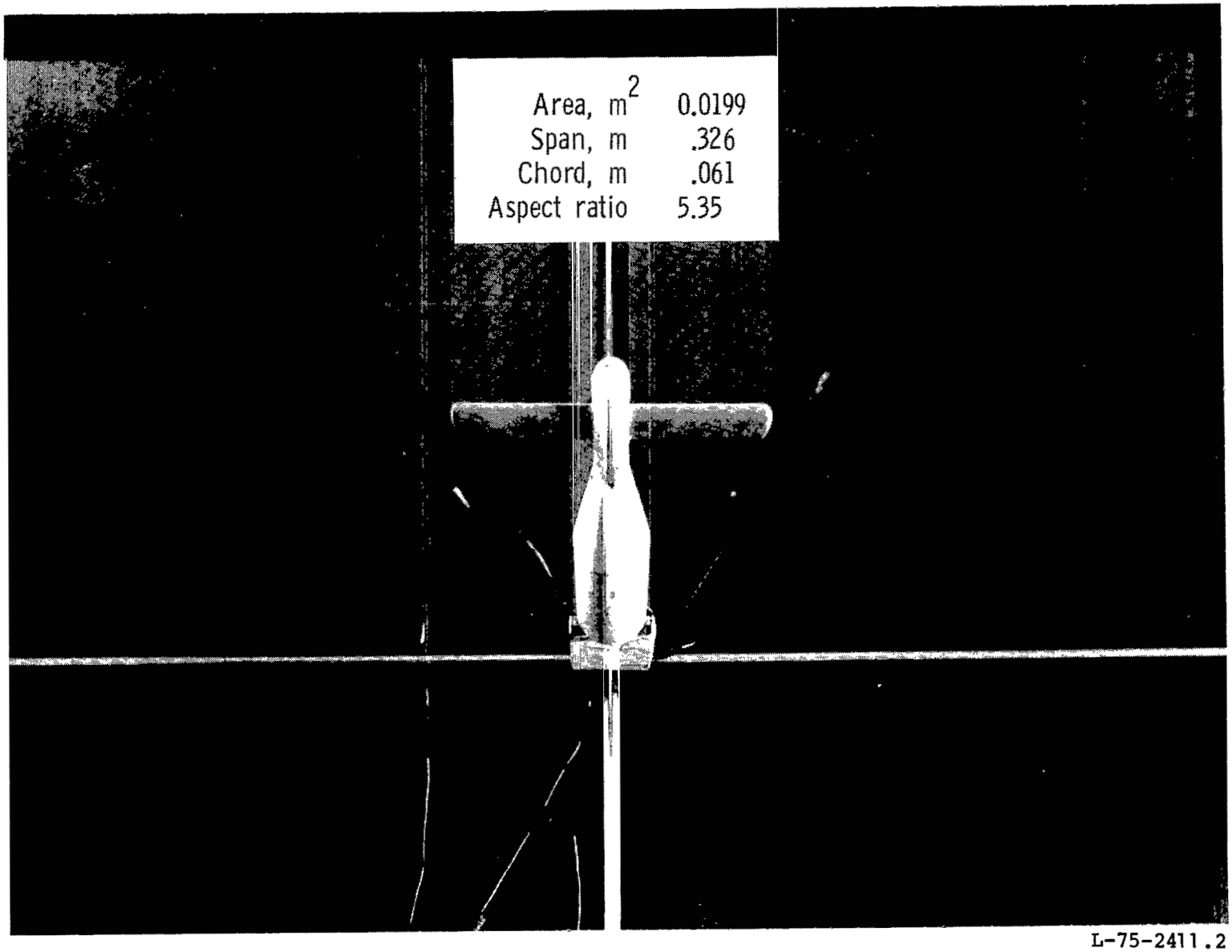

L-75-2411.2

Figure 5.- Photograph and dimensions of unswept trailing-wing model on traverse mechanism. Model has NACA 0012 airfoil section.

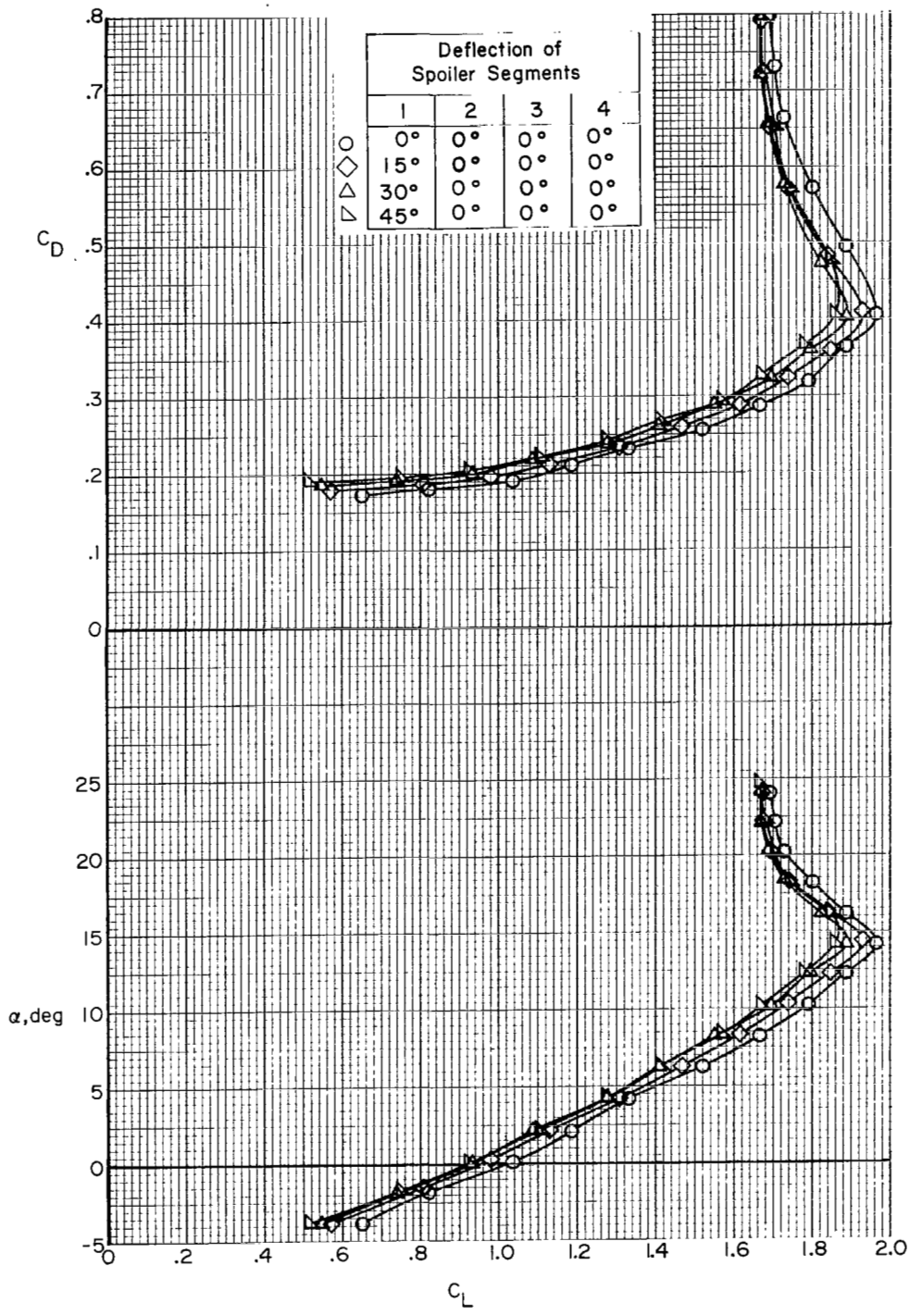

(a) Lift and drag coefficients.

Figure 6.- Effect of deflection angle of flight-spoiler segment 1 on longitudinal aerodynamic characteristics of transport aircraft model. $i_t = 0^o$; landing flap configuration; landing gear down.

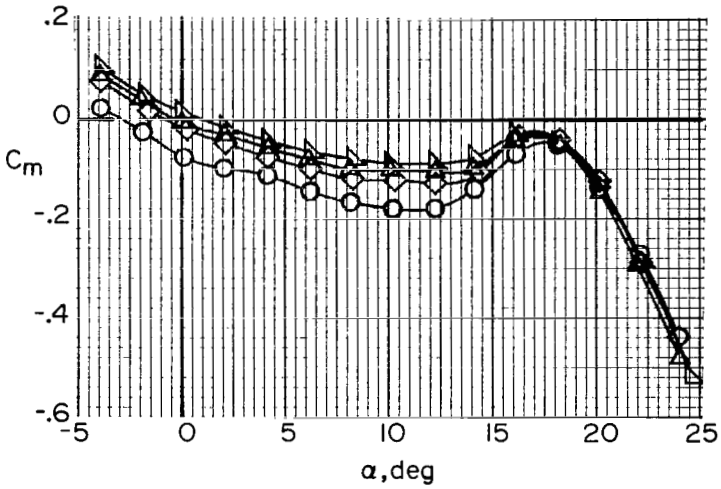

	Deflection of Spoiler Segments			
	1	2	3	4
○	0°	0°	0°	0°
◇	15°	0°	0°	0°
△	30°	0°	0°	0°
▷	45°	0°	0°	0°

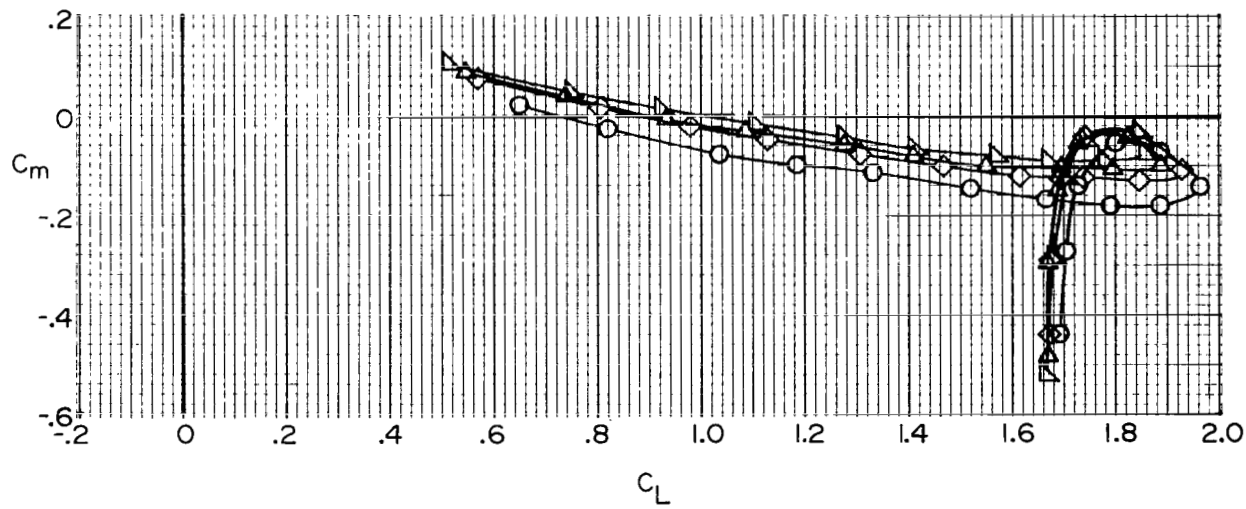

(b) Pitching-moment coefficient.

Figure 6.- Concluded.

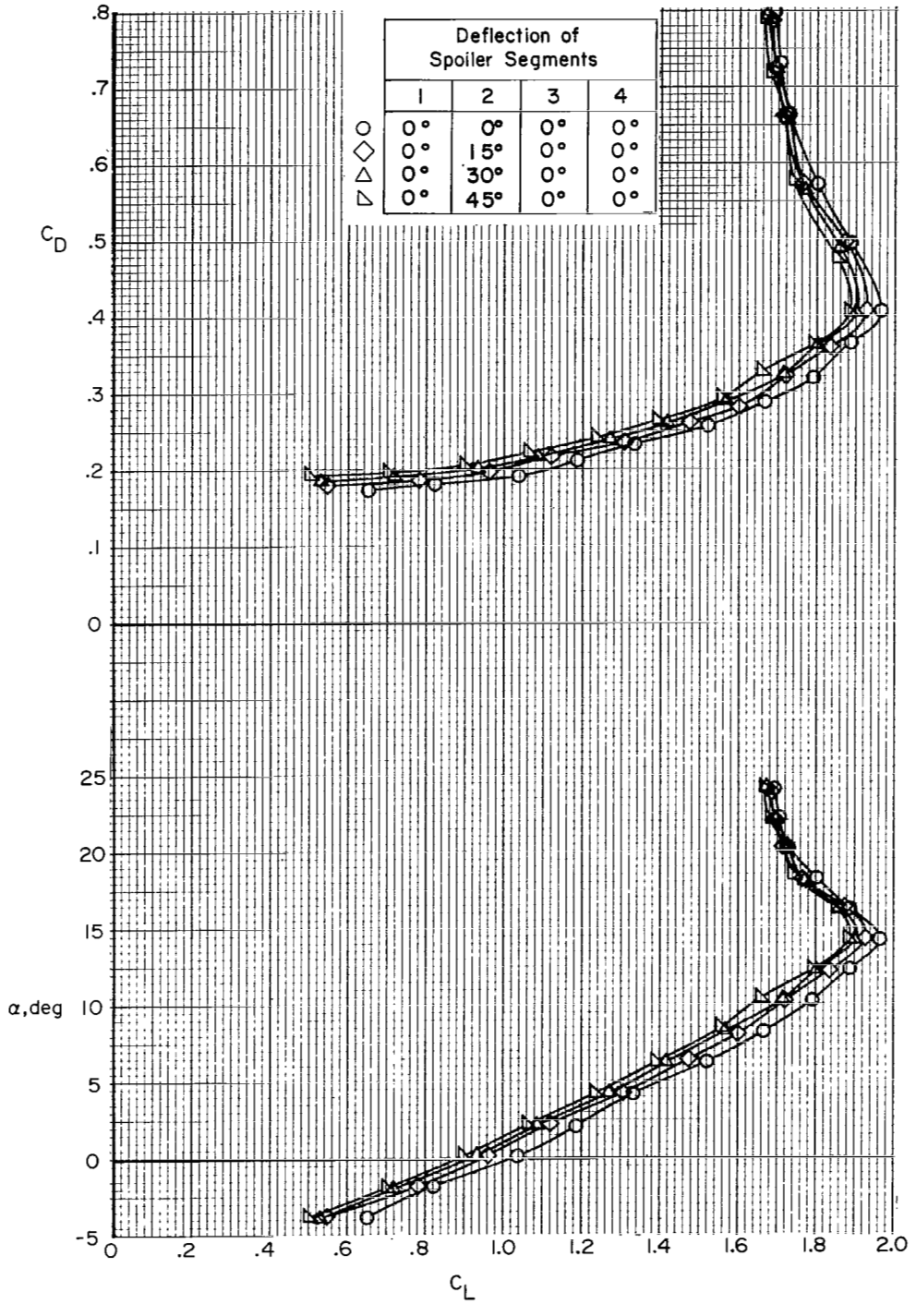

(a) Lift and drag coefficients.

Figure 7.- Effect of deflection angle of flight-spoiler segment 2 on longitudinal aerodynamic characteristics of transport aircraft model. $i_t = 0^o$; landing flap configuration; landing gear down.

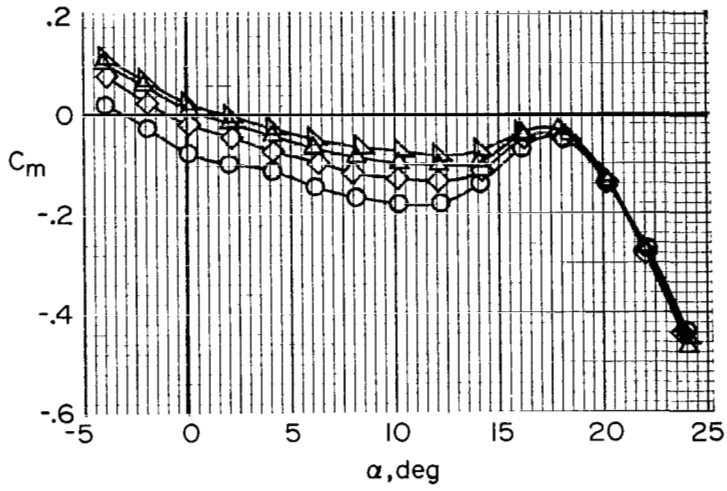

	Deflection of Spoiler Segments			
	1	2	3	4
○	0°	0°	0°	0°
◇	0°	15°	0°	0°
△	0°	30°	0°	0°
◺	0°	45°	0°	0°

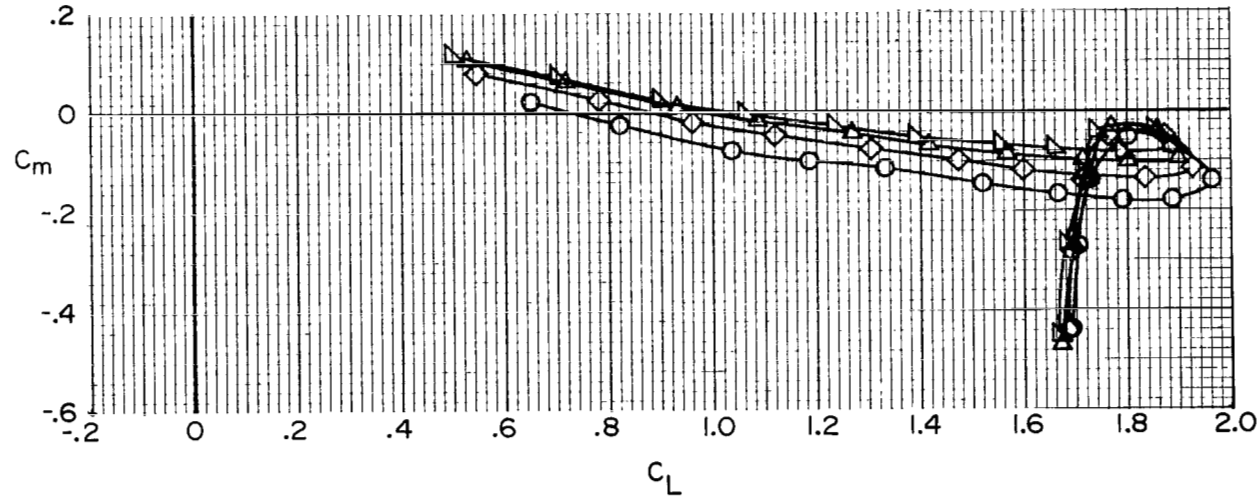

(b) Pitching-moment coefficient.

Figure 7.- Concluded.

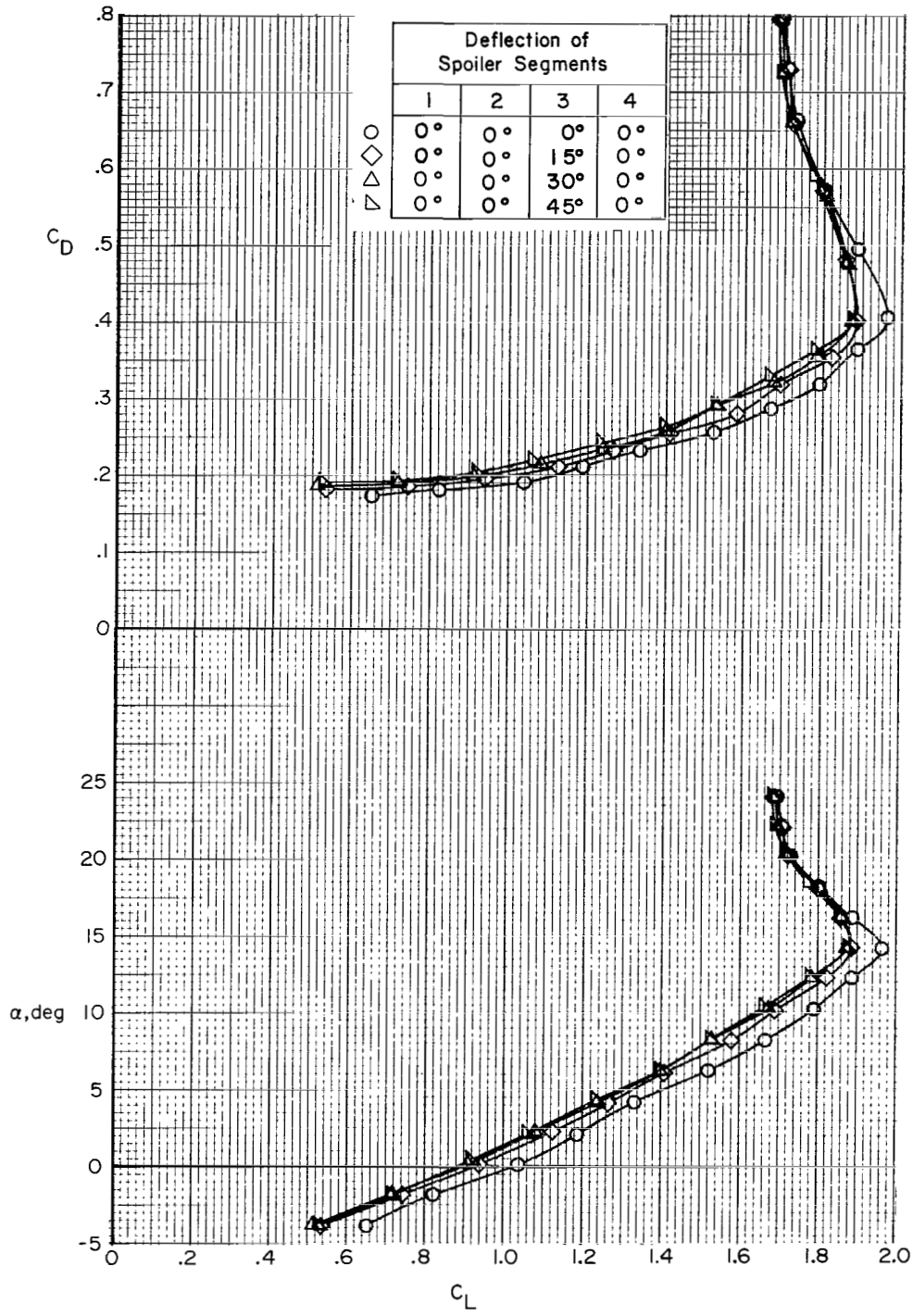

(a) Lift and drag coefficients.

Figure 8.- Effect of deflection angle of flight-spoiler segment 3 on longitudinal aerodynamic characteristics of transport aircraft model. $i_t = 0^o$; landing flap configuration; landing gear down.

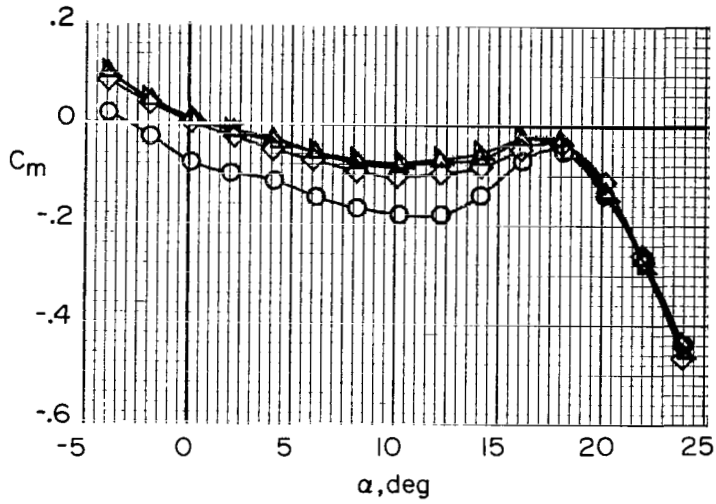

	Deflection of Spoiler Segments			
	1	2	3	4
○	0°	0°	0°	0°
◇	0°	0°	15°	0°
△	0°	0°	30°	0°
◺	0°	0°	45°	0°

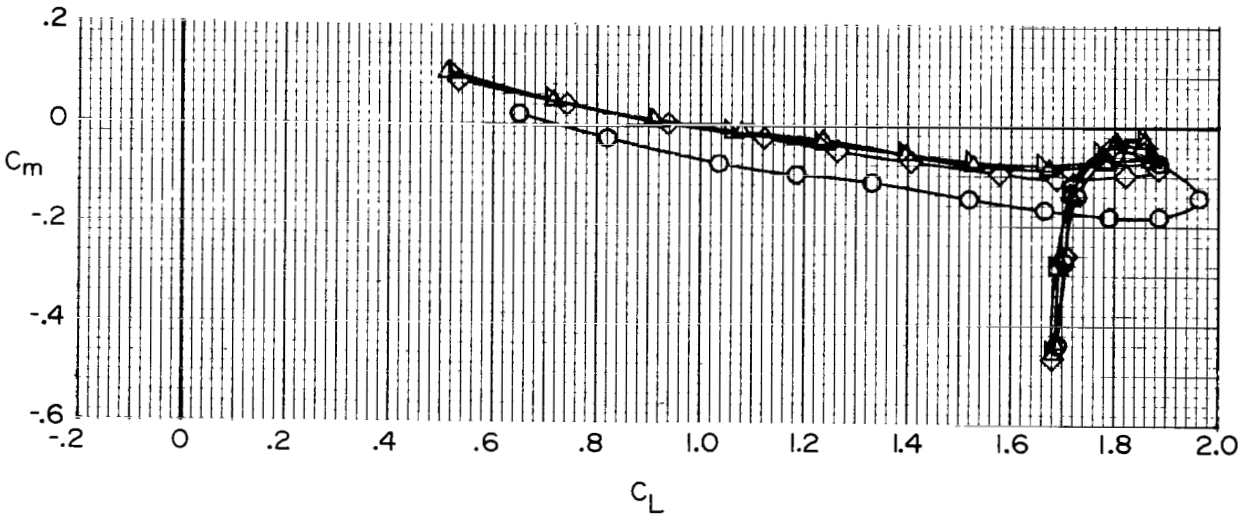

(b) Pitching-moment coefficient.

Figure 8.- Concluded.

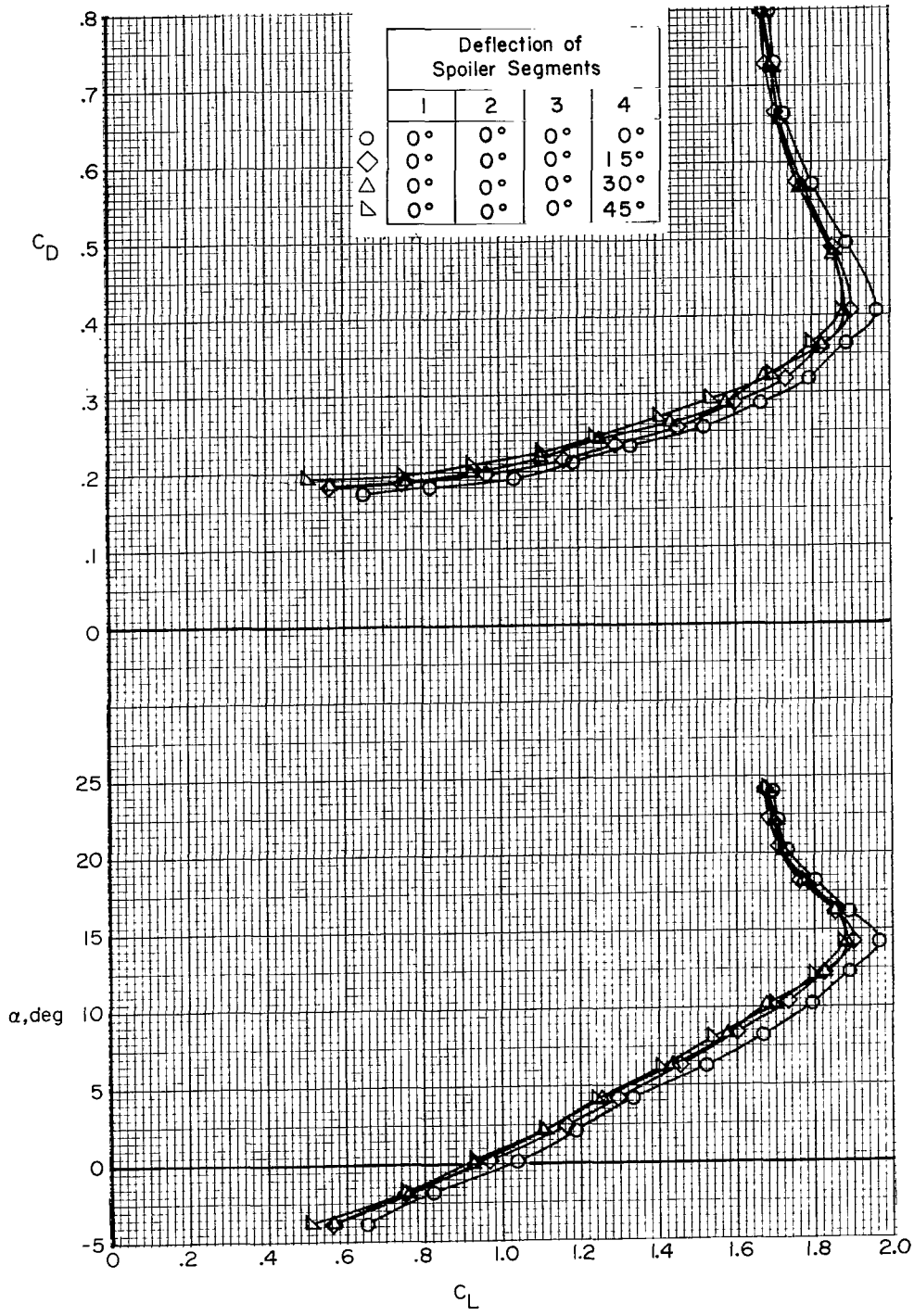

(a) Lift and drag coefficients.

Figure 9.- Effect of deflection angle of flight-spoiler segment 4 on longitudinal aerodynamic characteristics of transport aircraft model. $i_t = 0^o$; landing flap configuration; landing gear down.

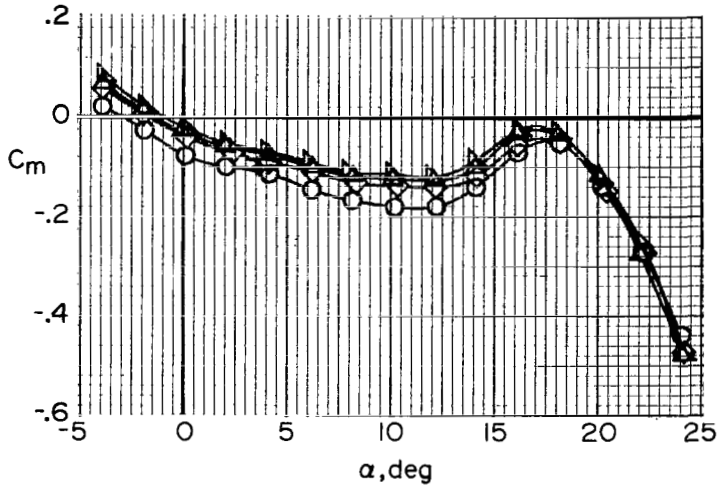

	Deflection of Spoiler Segments			
	1	2	3	4
○	0°	0°	0°	0°
◇	0°	0°	0°	15°
△	0°	0°	0°	30°
▷	0°	0°	0°	45°

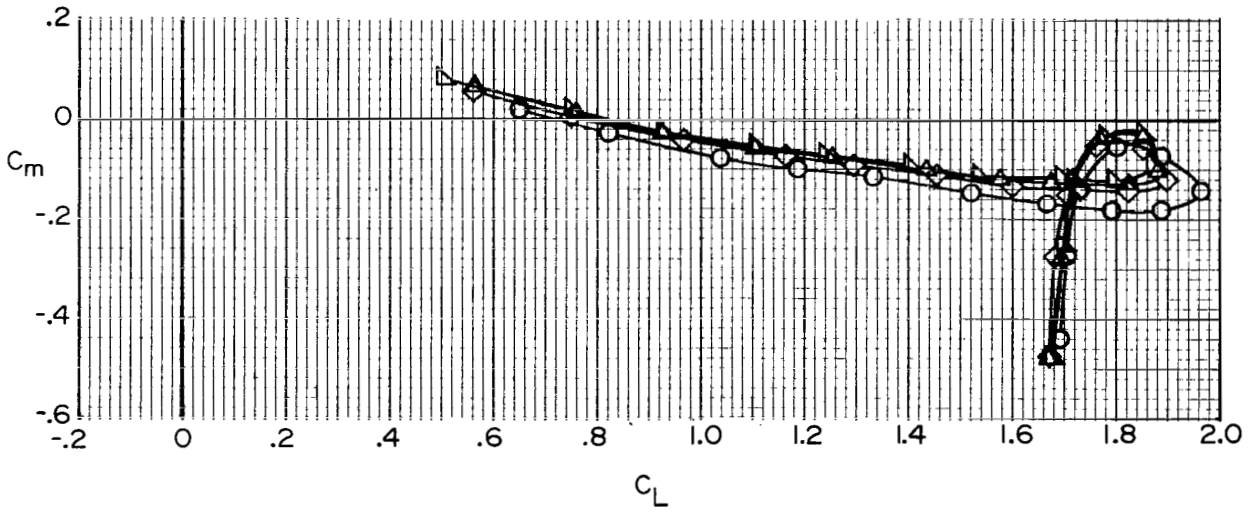

(b) Pitching-moment coefficient.

Figure 9.- Concluded.

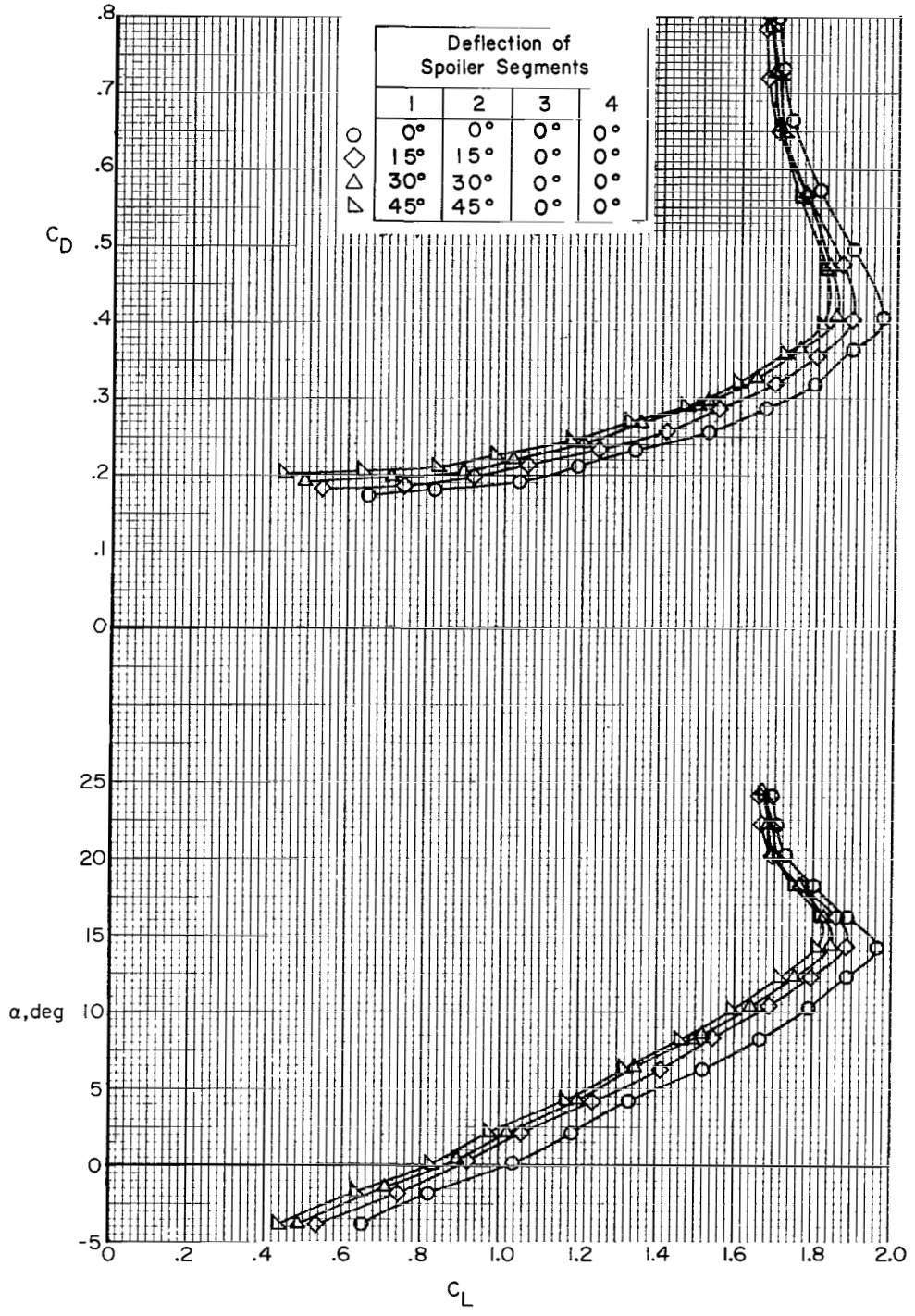

(a) Lift and drag coefficients.

Figure 10.- Effect of deflection angle of flight-spoiler segments 1 and 2 on longitudinal aerodynamic characteristics of transport aircraft model. $i_t = 0^o$; landing flap configuration; landing gear down.

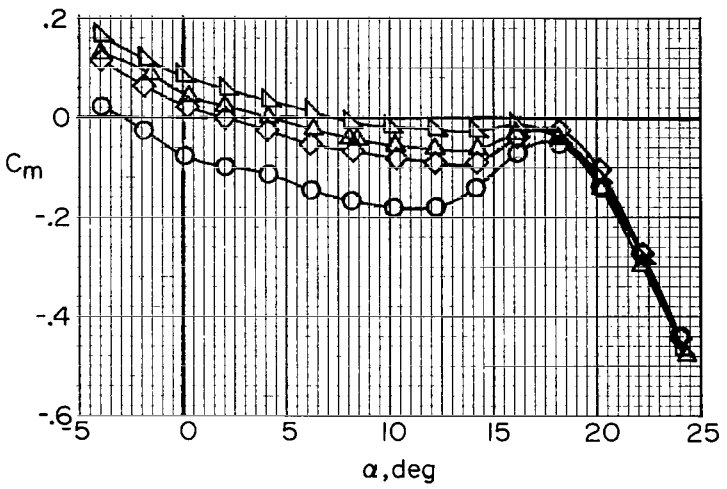

	Deflection of Spoiler Segments			
	1	2	3	4
○	0°	0°	0°	0°
◇	15°	15°	0°	0°
△	30°	30°	0°	0°
◺	45°	45°	0°	0°

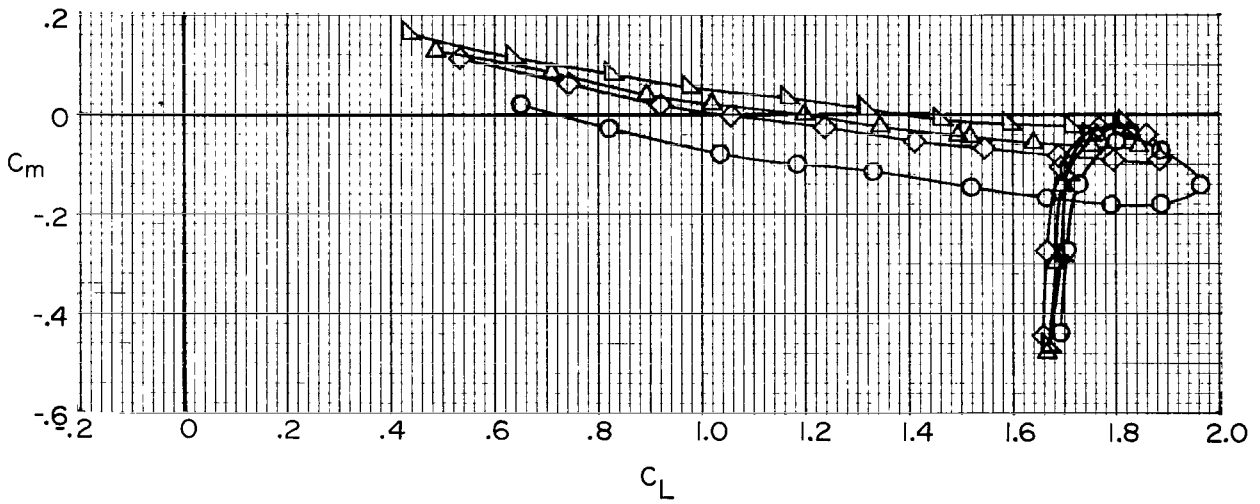

(b) Pitching-moment coefficient.

Figure 10.- Concluded.

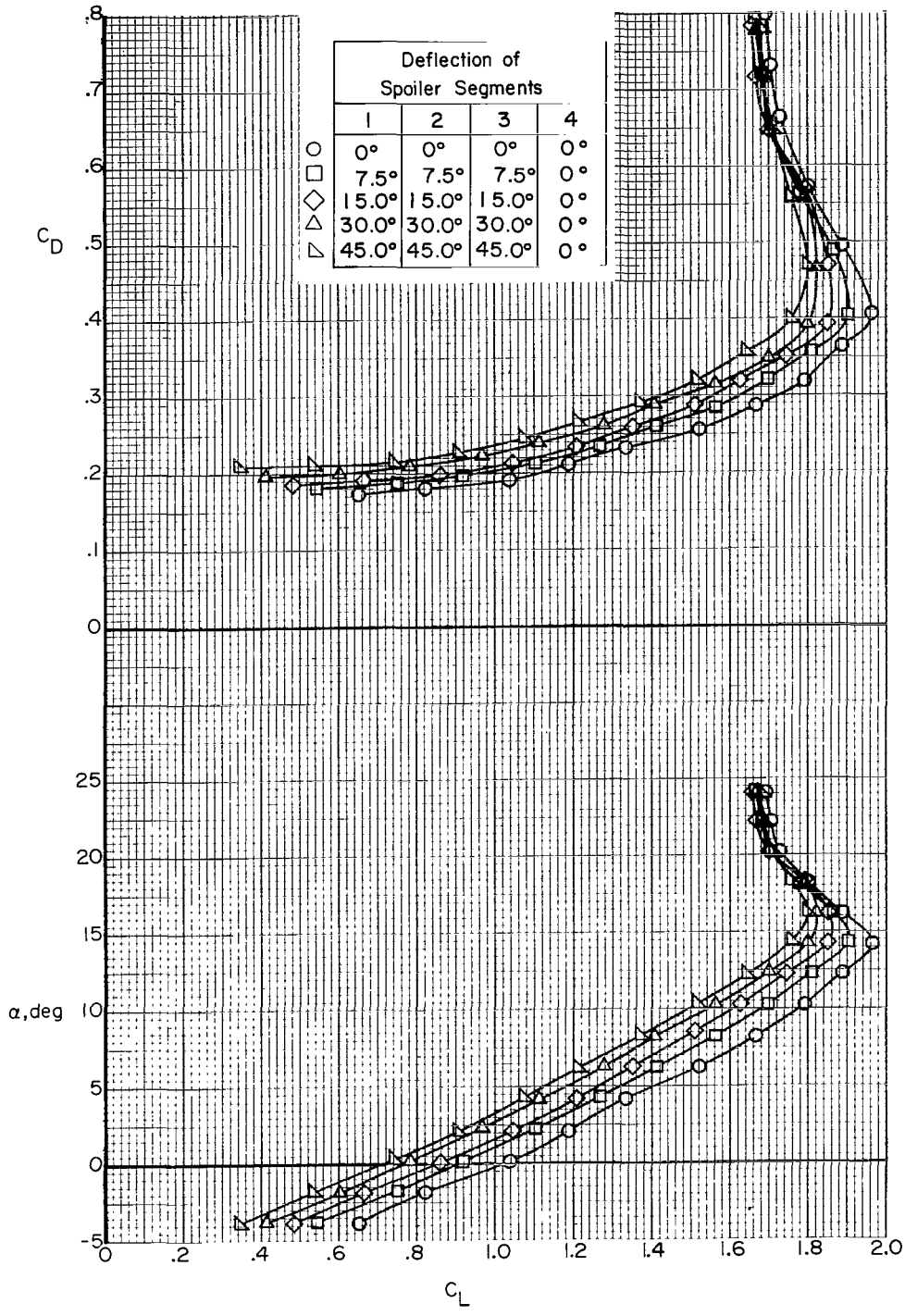

(a) Lift and drag coefficients.

Figure 11.- Effect of deflection angle of flight-spoiler segments 1, 2, and 3 on longitudinal aerodynamic characteristics of transport aircraft model. $i_t = 0^o$; landing flap configuration; landing gear down.

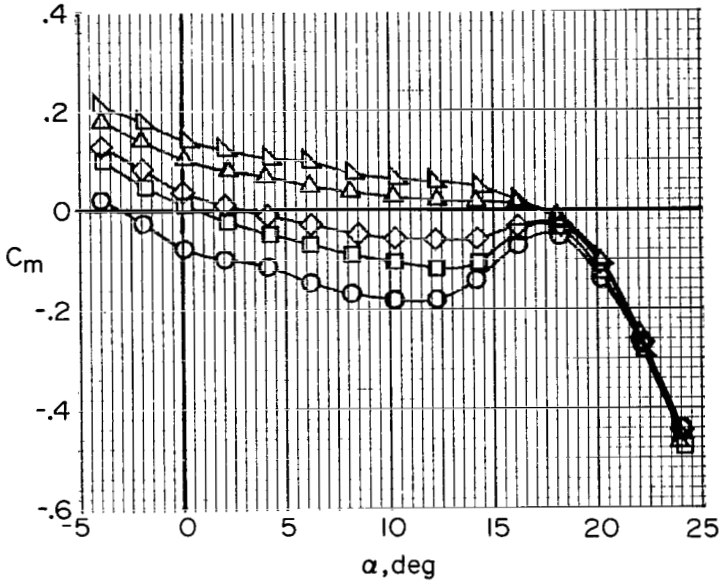

	Deflection of Spoiler Segments			
	1	2	3	4
○	0°	0°	0°	0°
□	7.5°	7.5°	7.5°	0°
◇	15.0°	15.0°	15.0°	0°
△	30.0°	30.0°	30.0°	0°
▷	45.0°	45.0°	45.0°	0°

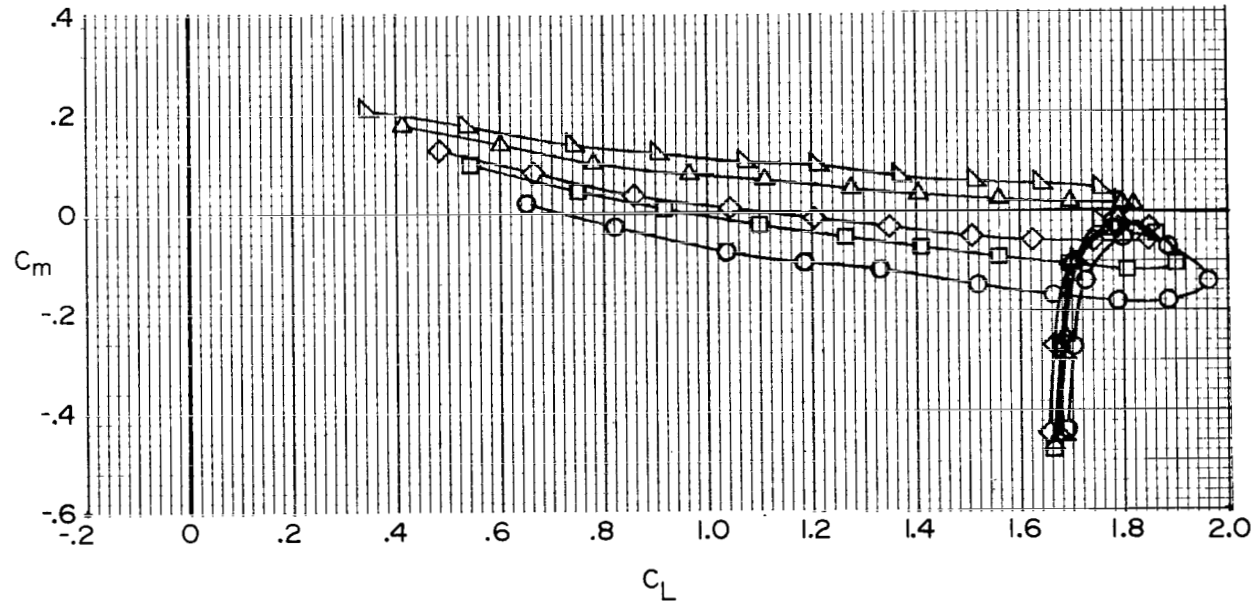

(b) Pitching-moment coefficient.

Figure 11.- Concluded.

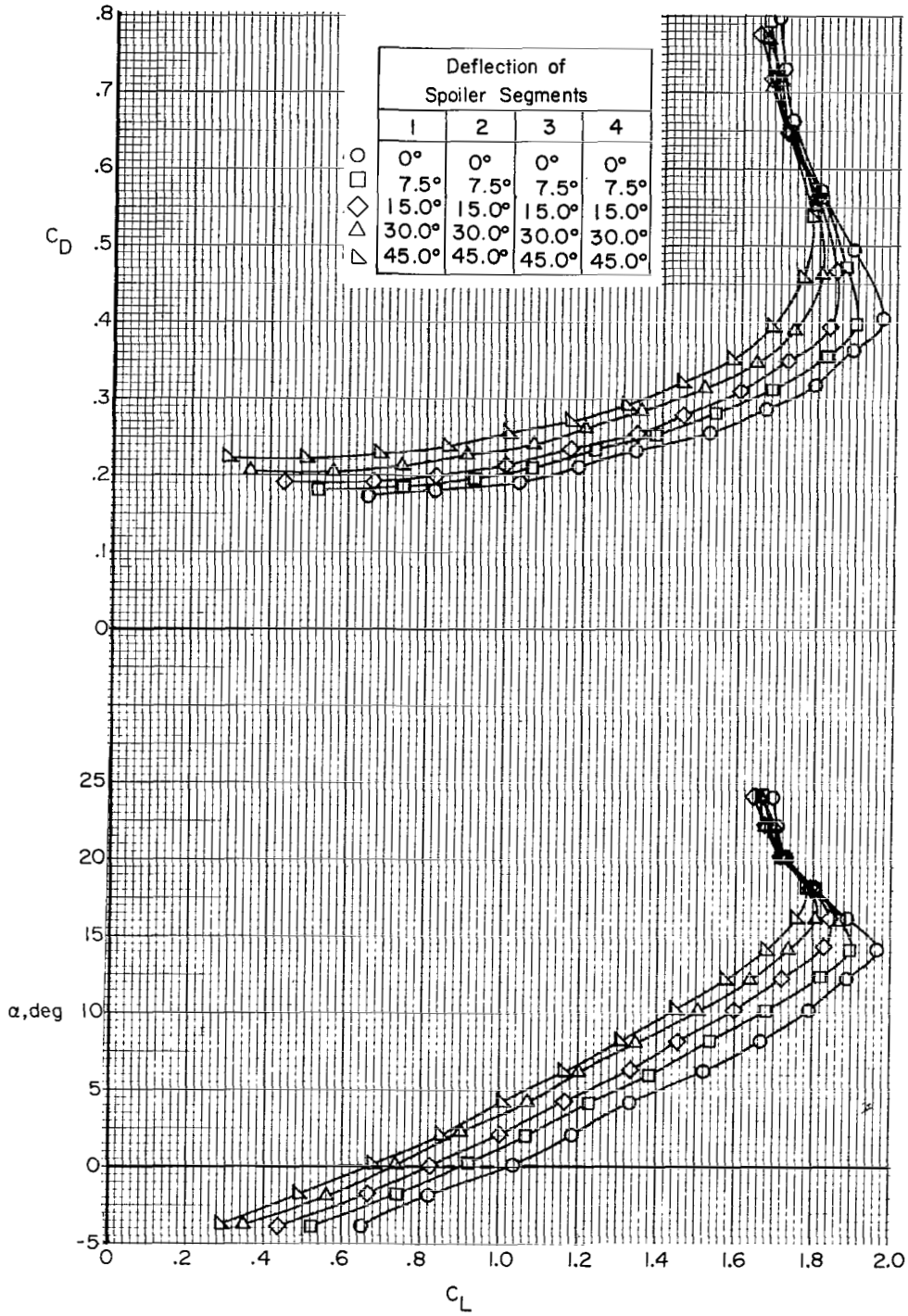

(a) Lift and drag coefficients.

Figure 12.- Effect of deflection angle of flight-spoiler segments 1, 2, 3, and 4 on longitudinal aerodynamic characteristics of transport aircraft model. $i_t = 0^o$; landing flap configuration; landing gear down.

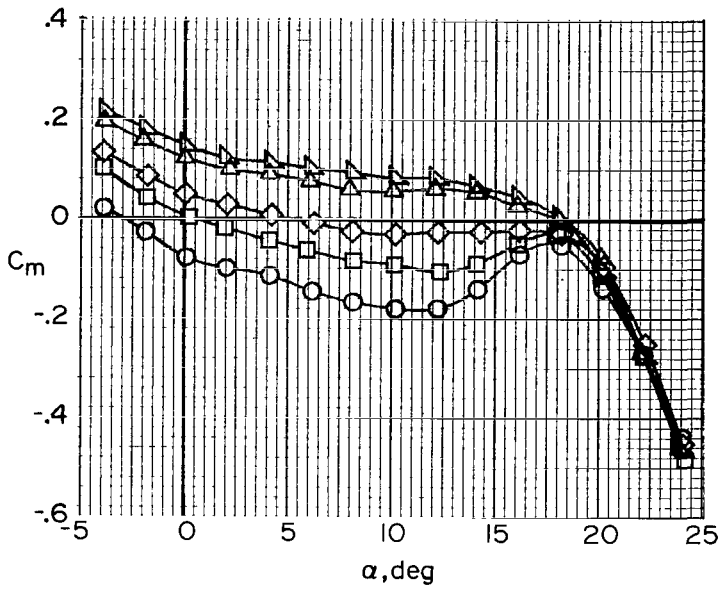

	Deflection of Spoiler Segments			
	1	2	3	4
○	0°	0°	0°	0°
□	7.5°	7.5°	7.5°	7.5°
◇	15.0°	15.0°	15.0°	15.0°
△	30.0°	30.0°	30.0°	30.0°
◺	45.0°	45.0°	45.0°	45.0°

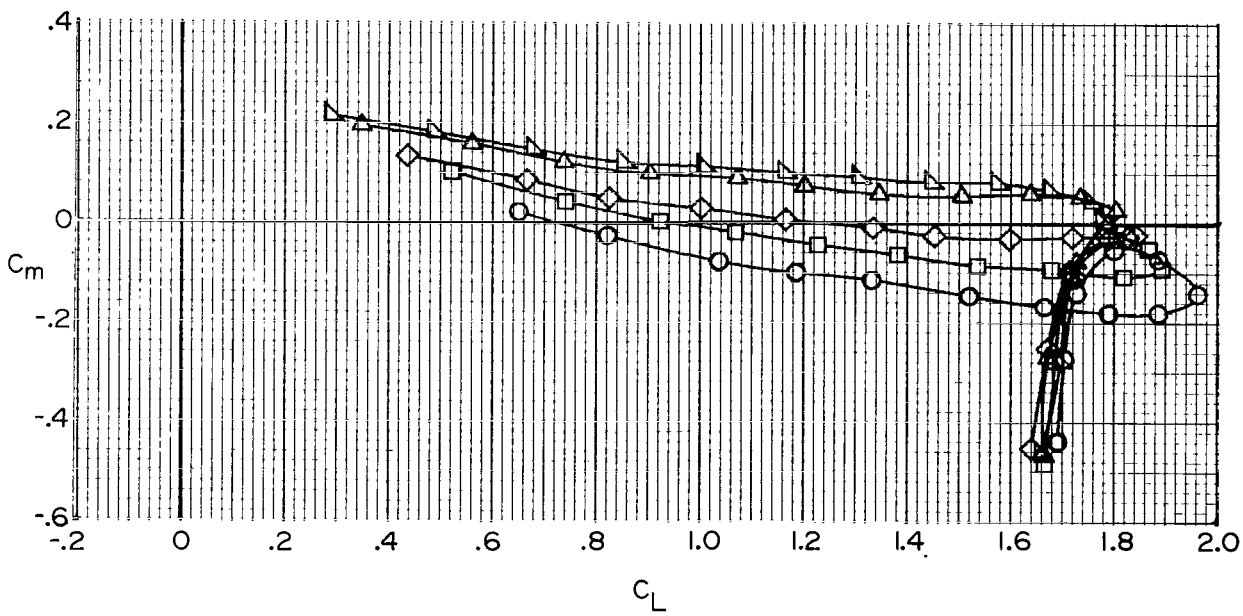

(b) Pitching-moment coefficient.

Figure 12.- Concluded.

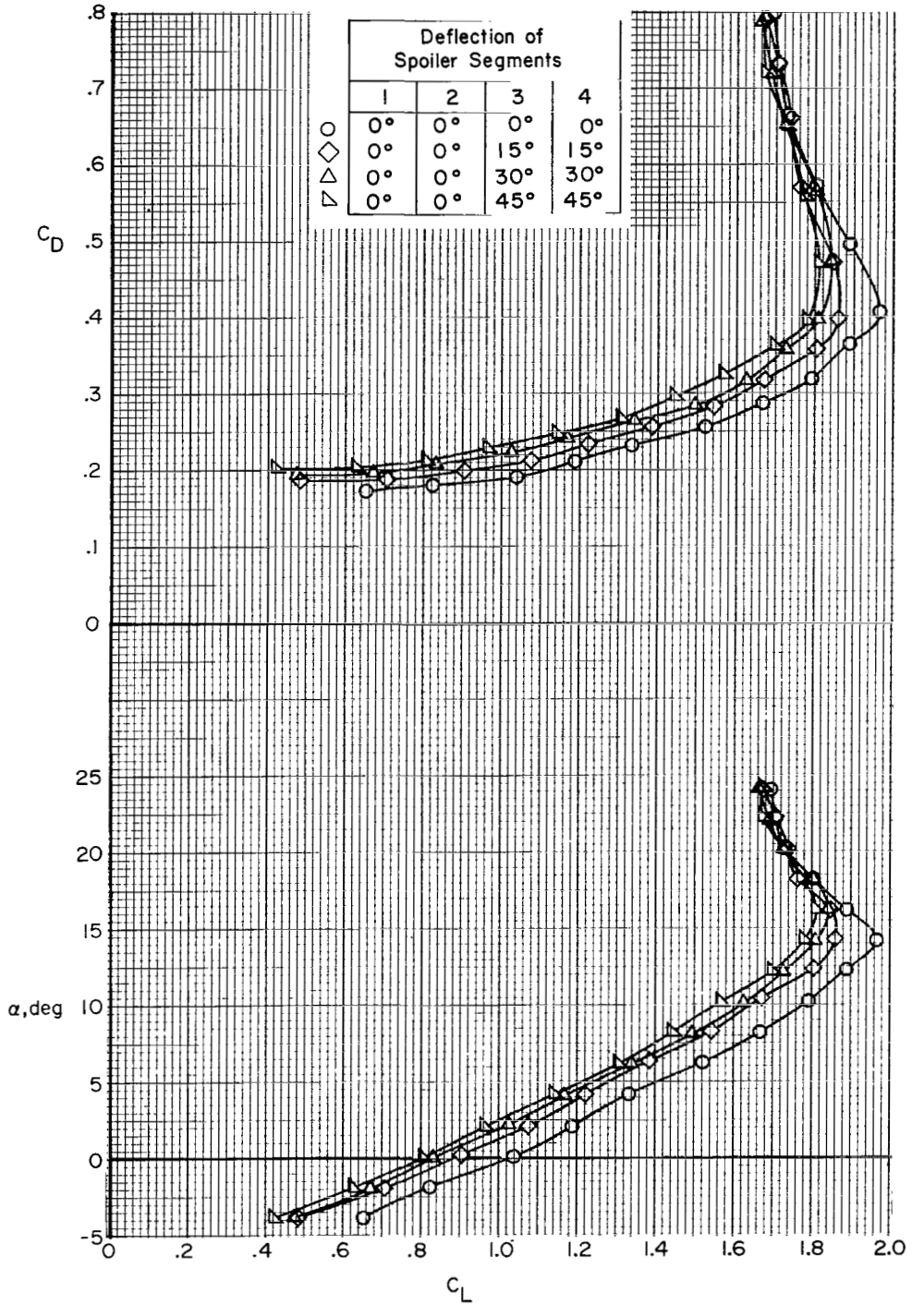

(a) Lift and drag coefficients.

Figure 13.- Effect of deflection angle of flight-spoiler segments 3 and 4 on longitudinal aerodynamic characteristics of transport aircraft model. $i_t = 0^o$; landing flap configuration; landing gear down.

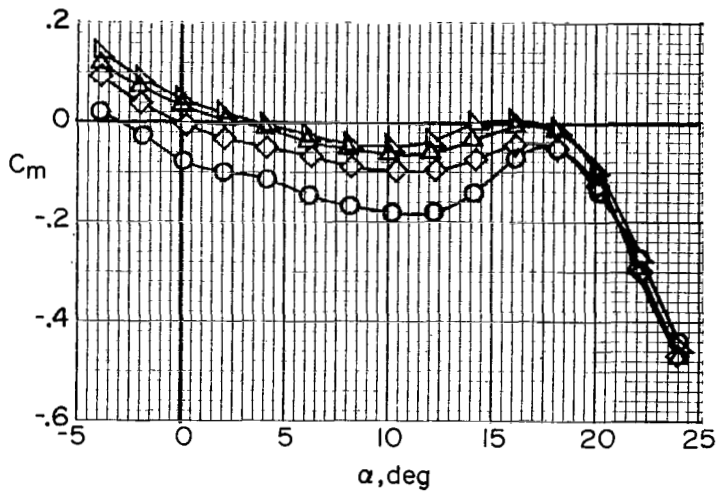

	Deflection of Spoiler Segments			
	1	2	3	4
○	0°	0°	0°	0°
◇	0°	0°	15°	15°
△	0°	0°	30°	30°
▷	0°	0°	45°	45°

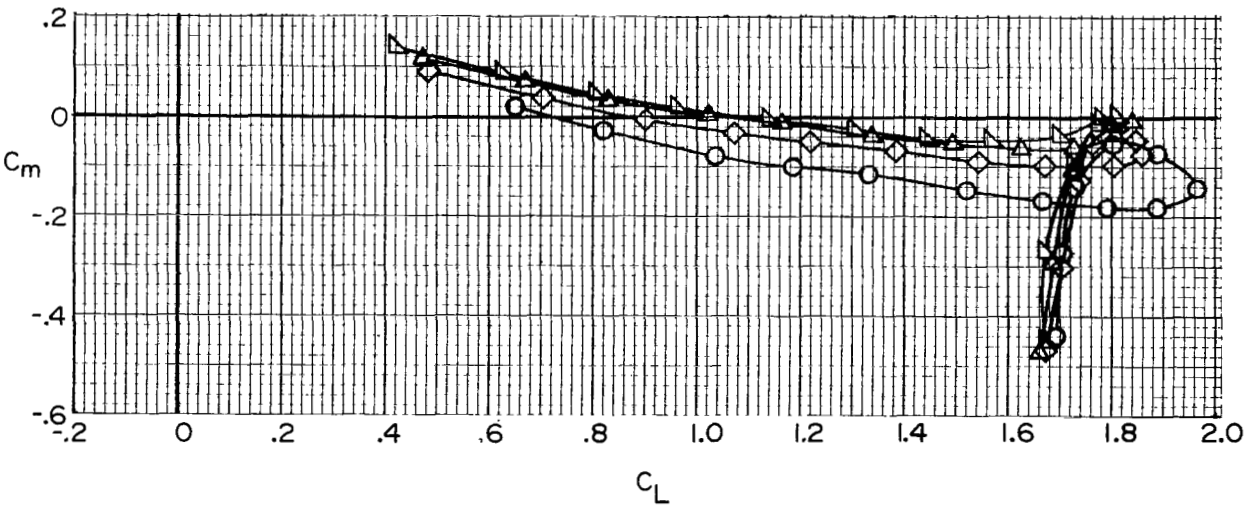

(b) Pitching–moment coefficient.

Figure 13.- Concluded.

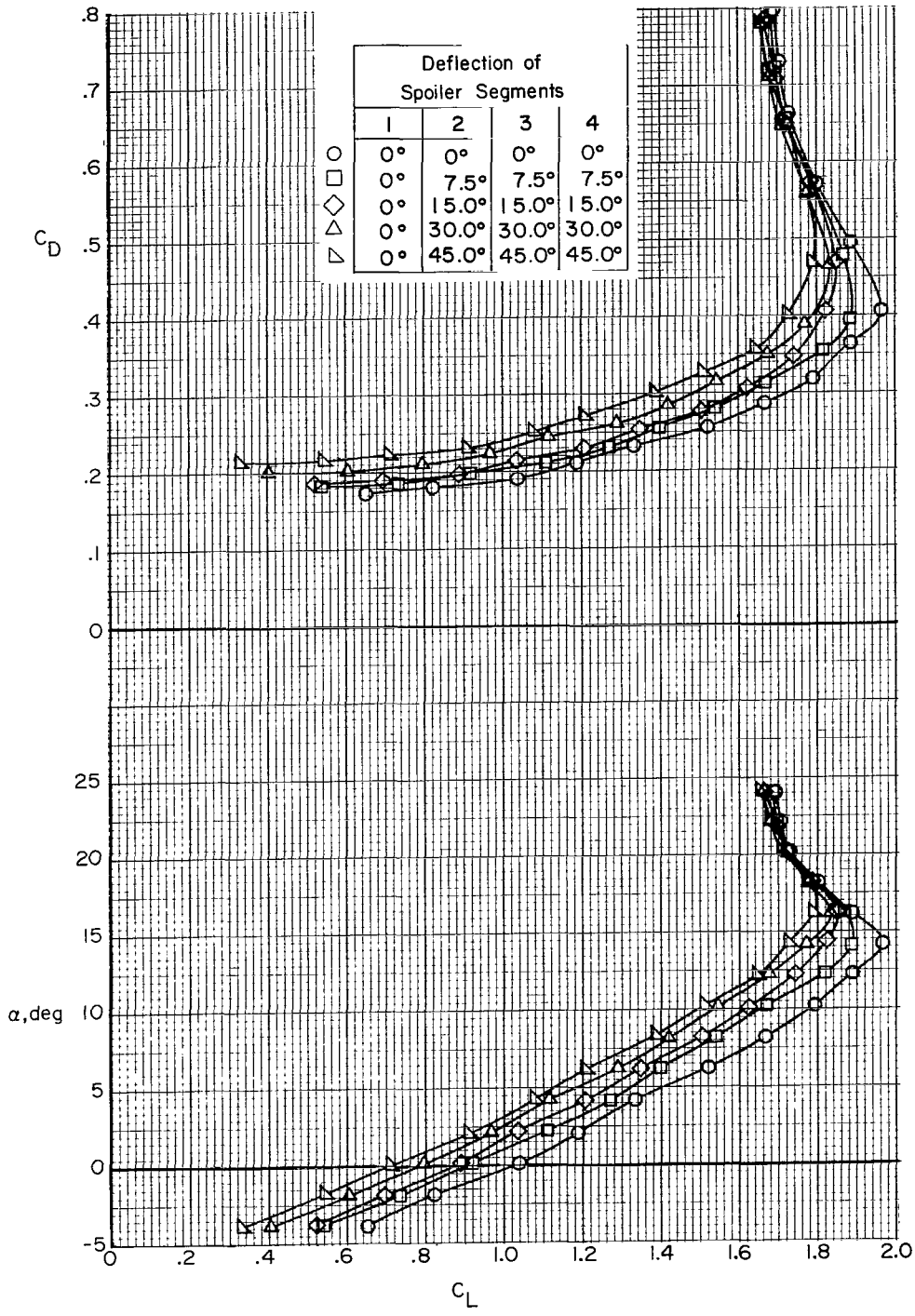

(a) Lift and drag coefficients.

Figure 14.- Effect of deflection angle of flight-spoiler segments 2, 3, and 4 on longitudinal aerodynamic characteristics of transport aircraft model. $i_t = 0^o$; landing flap configuration; landing gear down.

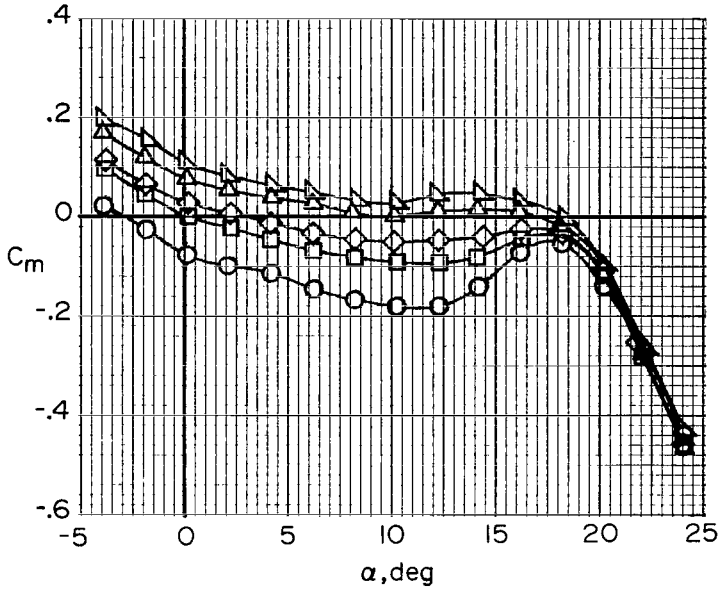

	Deflection of Spoiler Segments			
	1	2	3	4
○	0°	0°	0°	0°
□	0°	7.5°	7.5°	7.5°
◇	0°	15.0°	15.0°	15.0°
△	0°	30.0°	30.0°	30.0°
▷	0°	45.0°	45.0°	45.0°

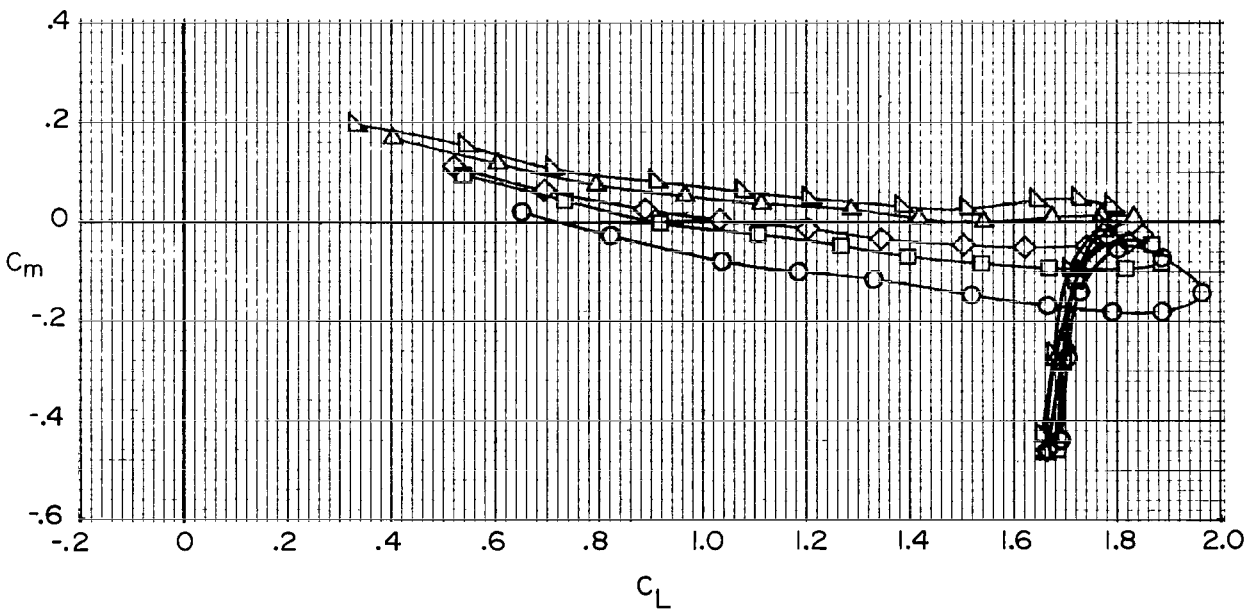

(b) Pitching-moment coefficient.

Figure 14.- Concluded.

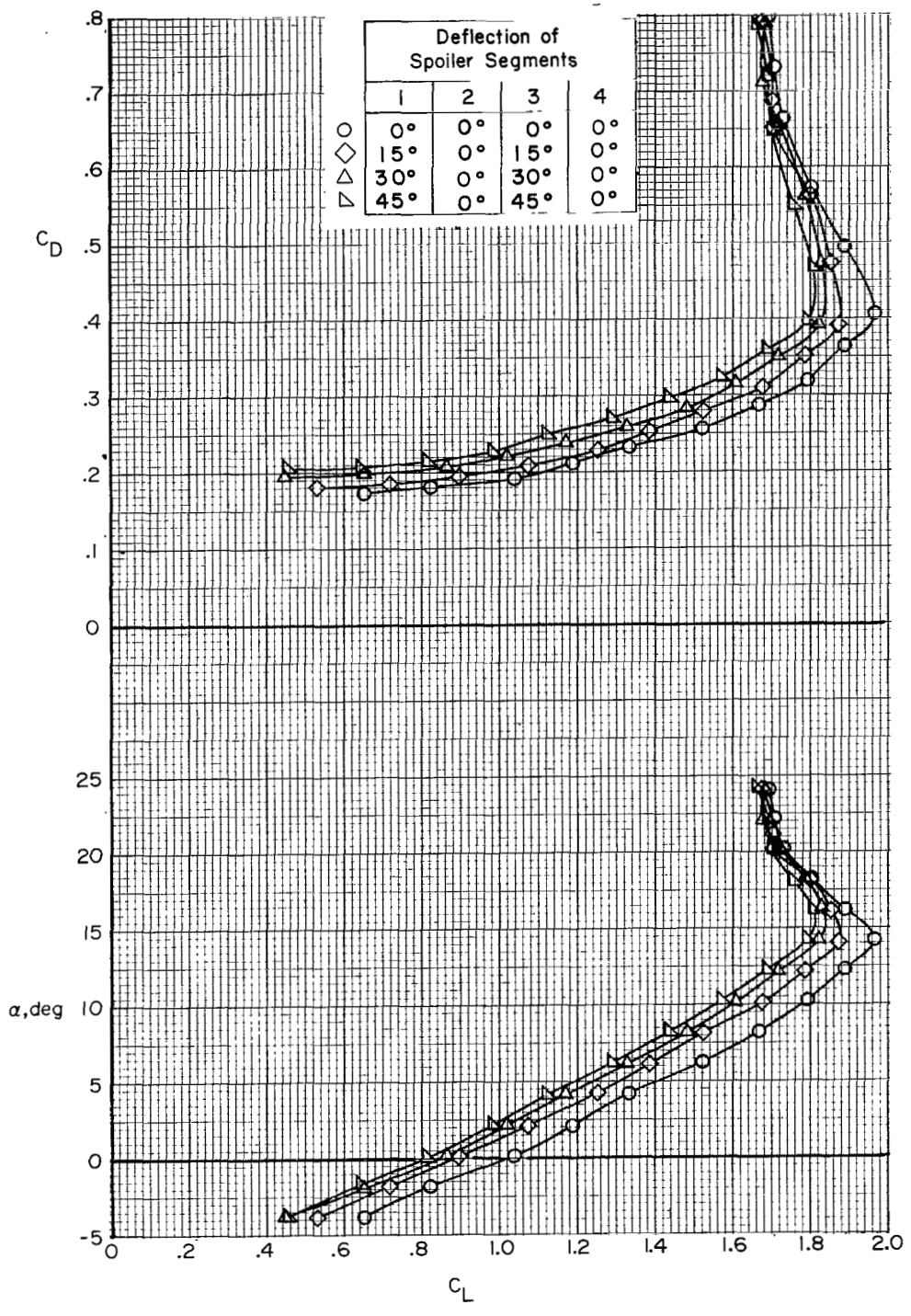

(a) Lift and drag coefficients.

Figure 15.- Effect of deflection angle of flight-spoiler segments 1 and 3 on longitudinal aerodynamic characteristics of transport aircraft model. $i_t = 0^o$; landing flap configuration; landing gear down.

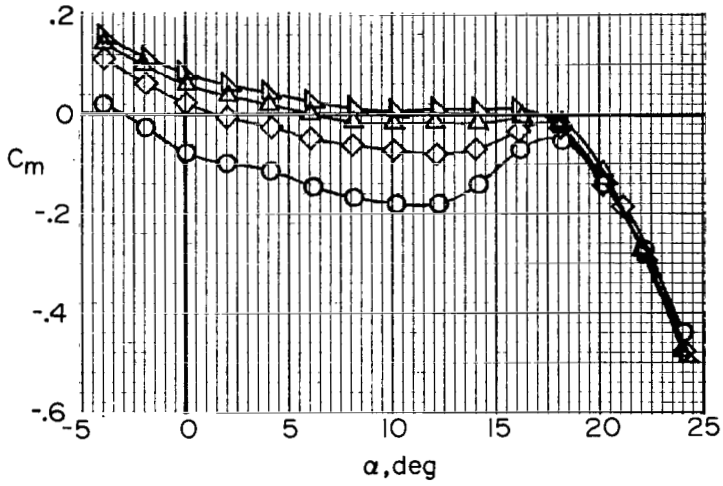

	Deflection of Spoiler Segments			
	1	2	3	4
○	0°	0°	0°	0°
◇	15°	0°	15°	0°
△	30°	0°	30°	0°
▷	45°	0°	45°	0°

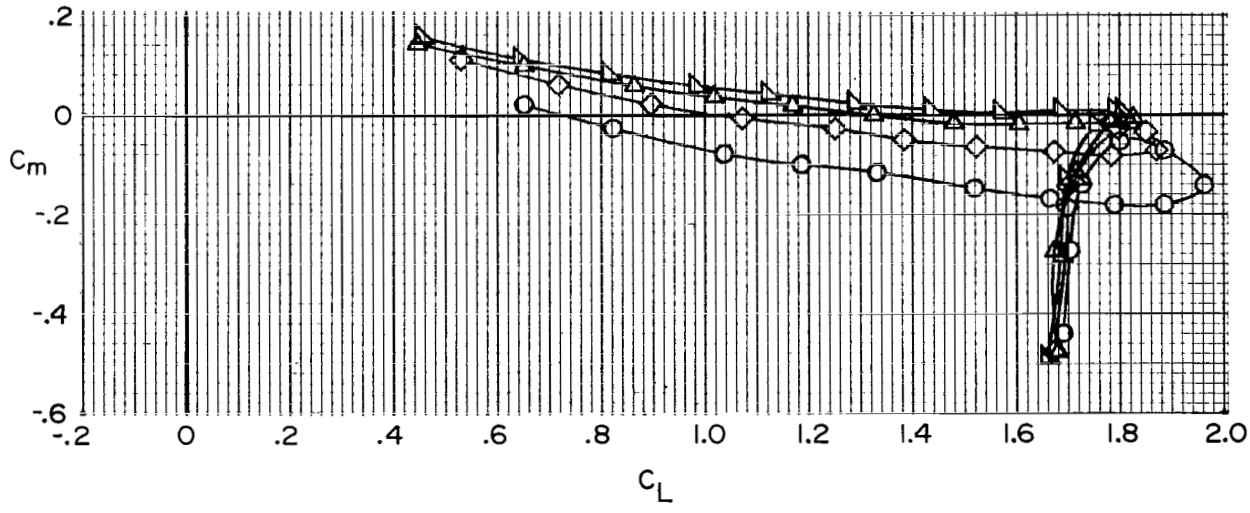

(b) Pitching-moment coefficient.

Figure 15.- Concluded.

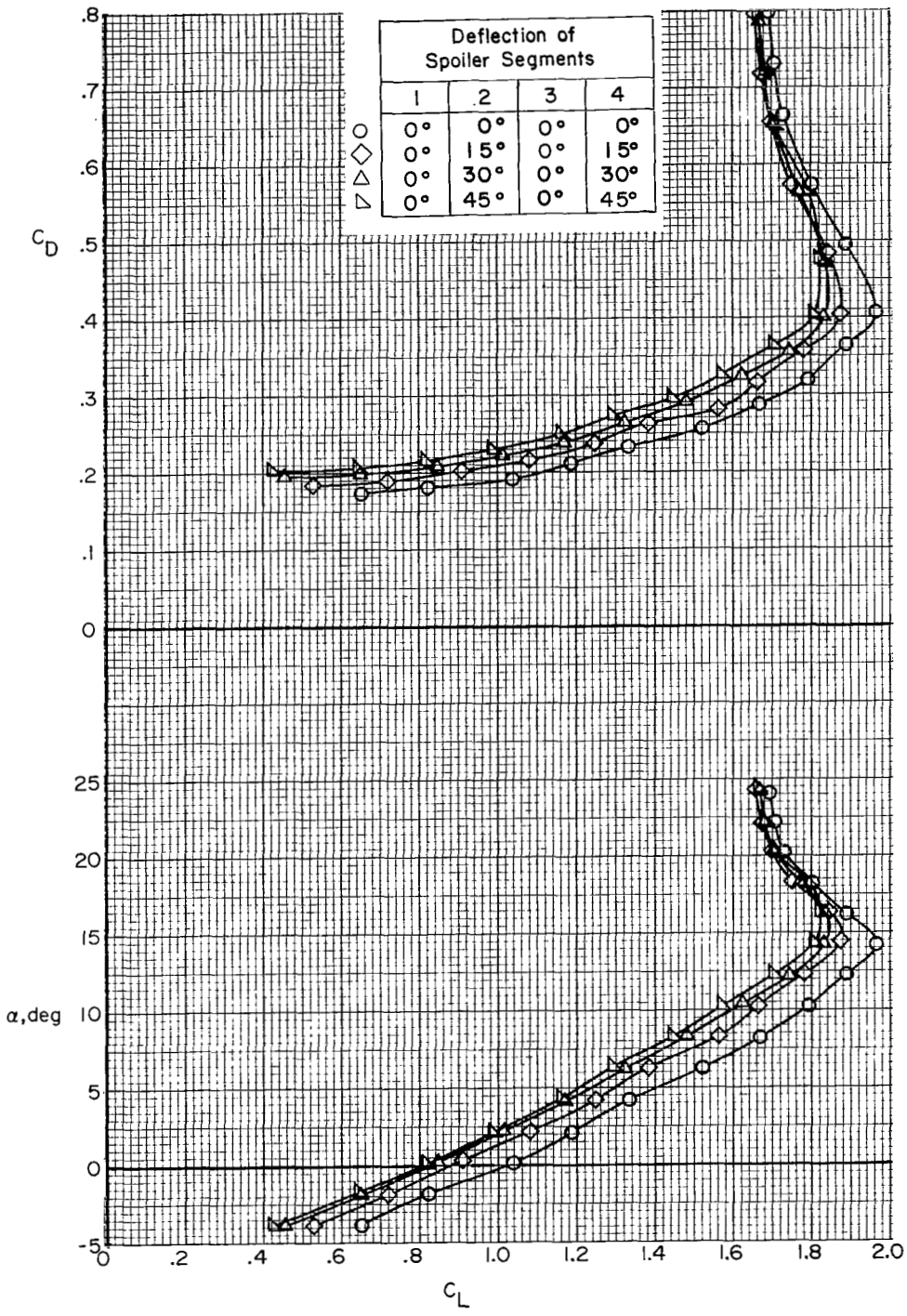

(a) Lift and drag coefficients.

Figure 16.- Effect of deflection angle of flight-spoiler segments 2 and 4 on longitudinal aerodynamic characteristics of transport aircraft model. $i_t = 0^o$; landing flap configuration; landing gear down.

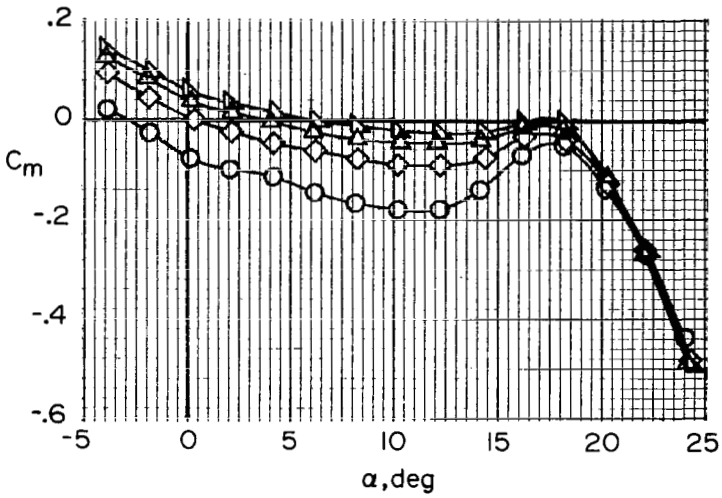

	Deflection of Spoiler Segments			
	1	2	3	4
○	0°	0°	0°	0°
◇	0°	15°	0°	15°
△	0°	30°	0°	30°
◁	0°	45°	0°	45°

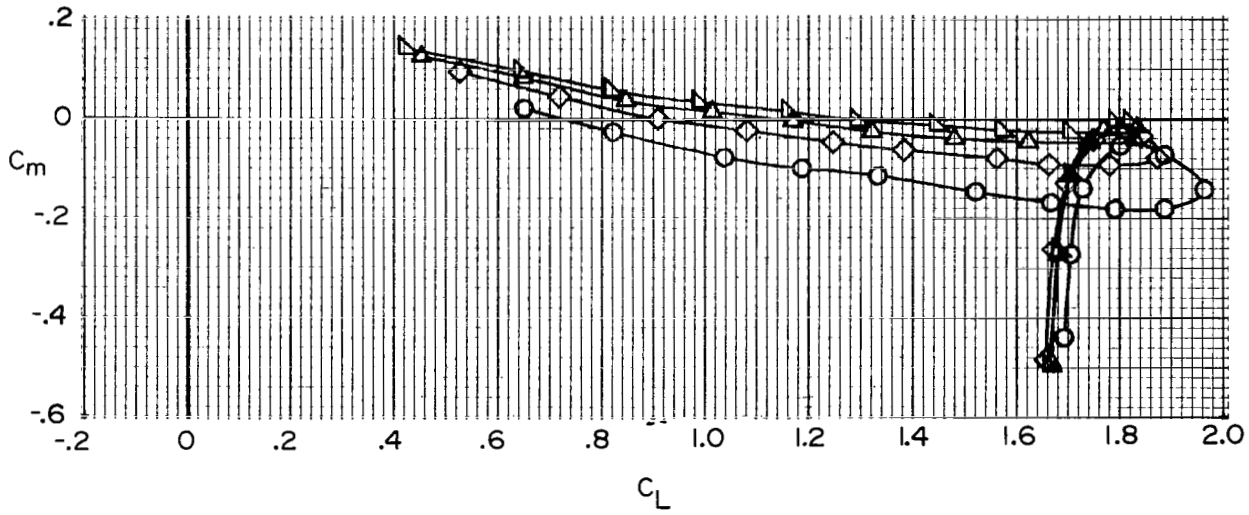

(b) Pitching-moment coefficient.

Figure 16.- Concluded.

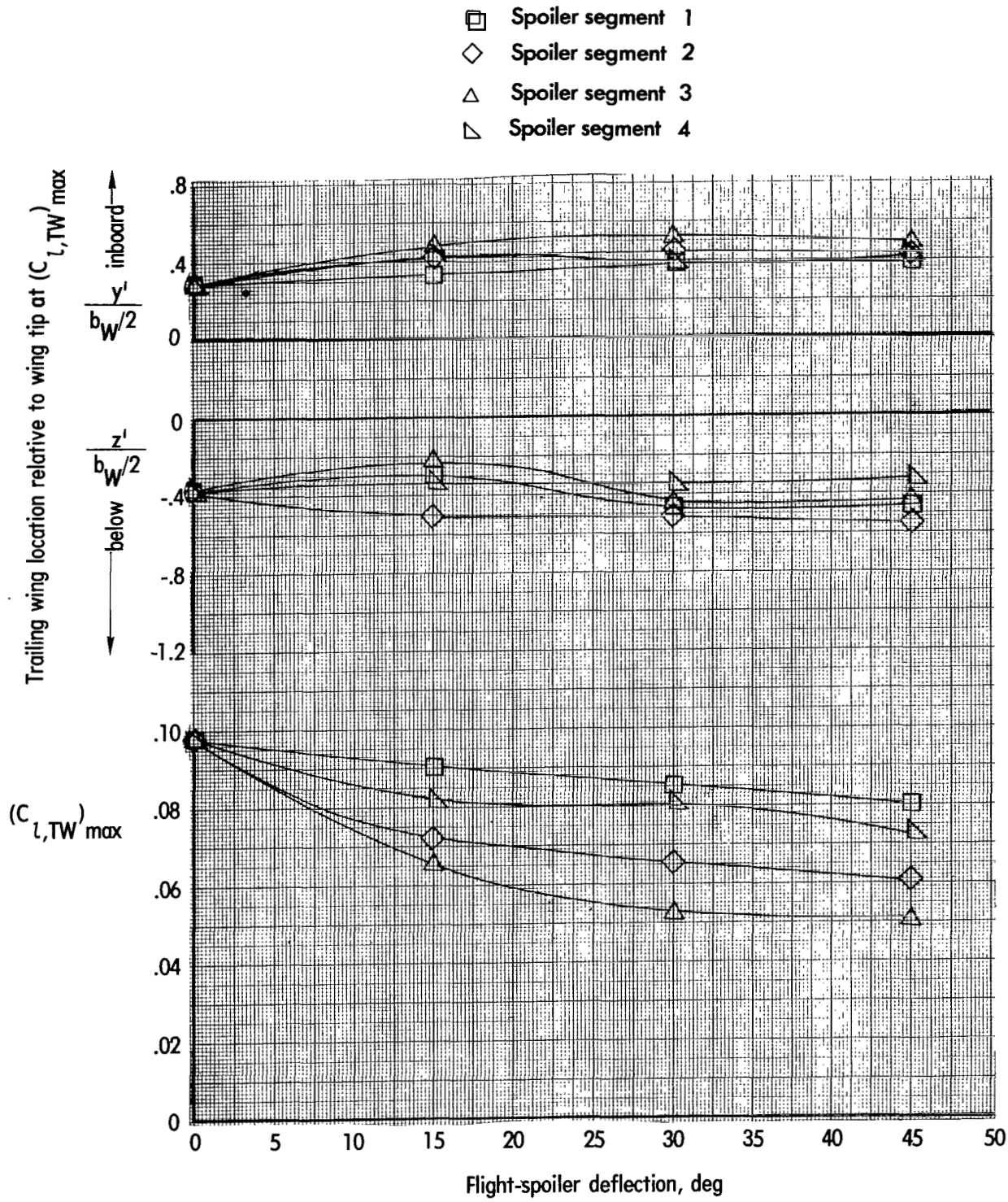

Figure 17.- Variation of trailing-wing location and rolling-moment coefficient with flight-spoiler deflection for flight-spoiler segments 1; 2; 3; and 4. Trailing-wing model located 7.8 transport wing spans behind transport aircraft model; $C_{L,trim} = 1.2$.

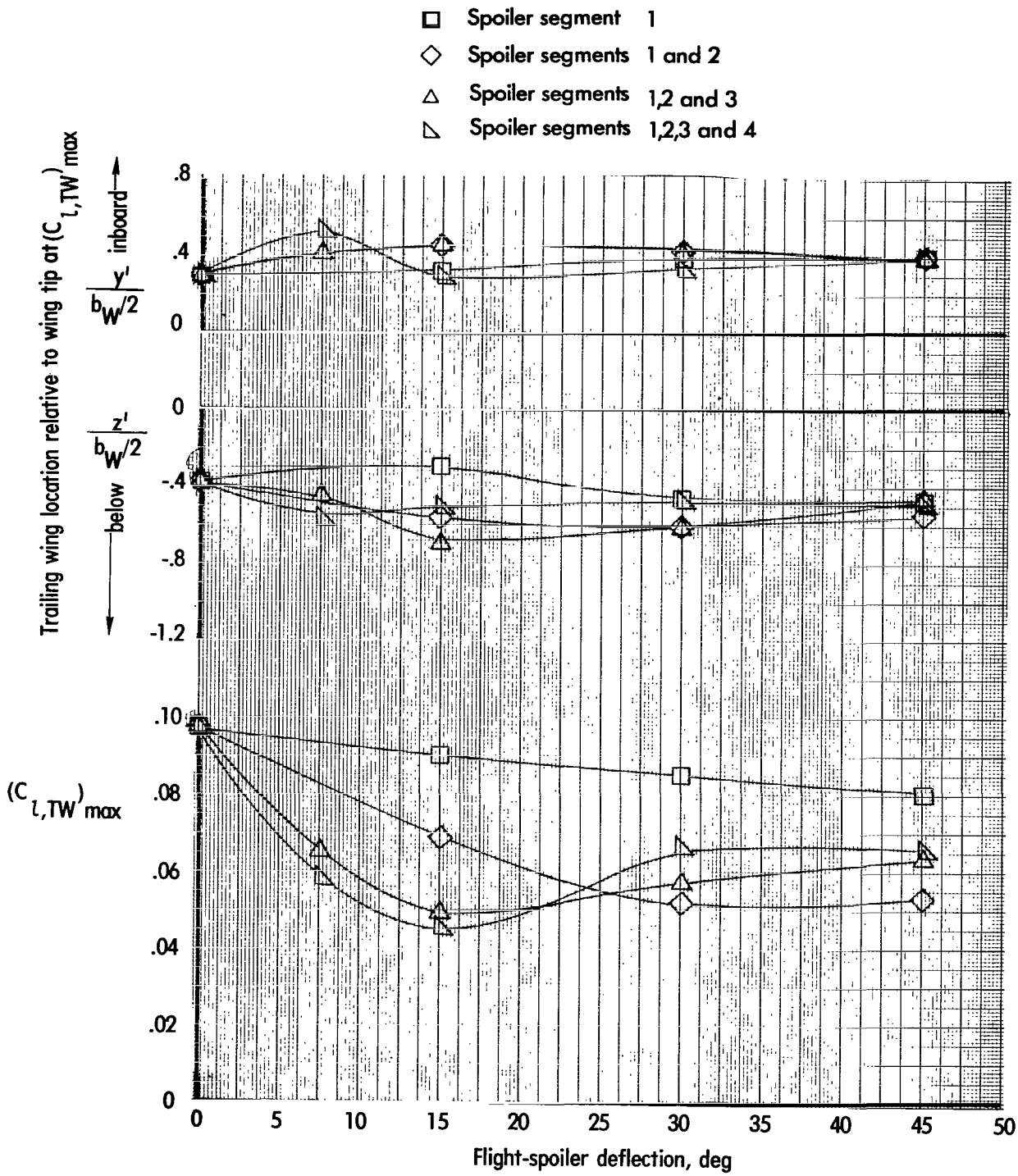

Figure 18.- Variation of trailing wing location and rolling-moment coefficient with flight-spoiler deflection for flight-spoiler segments 1; 1 and 2; 1, 2, and 3; 1, 2, 3, and 4. Trailing wing model located 7.8 transport wing spans behind transport aircraft model; $C_{L,trim} = 1.2$.

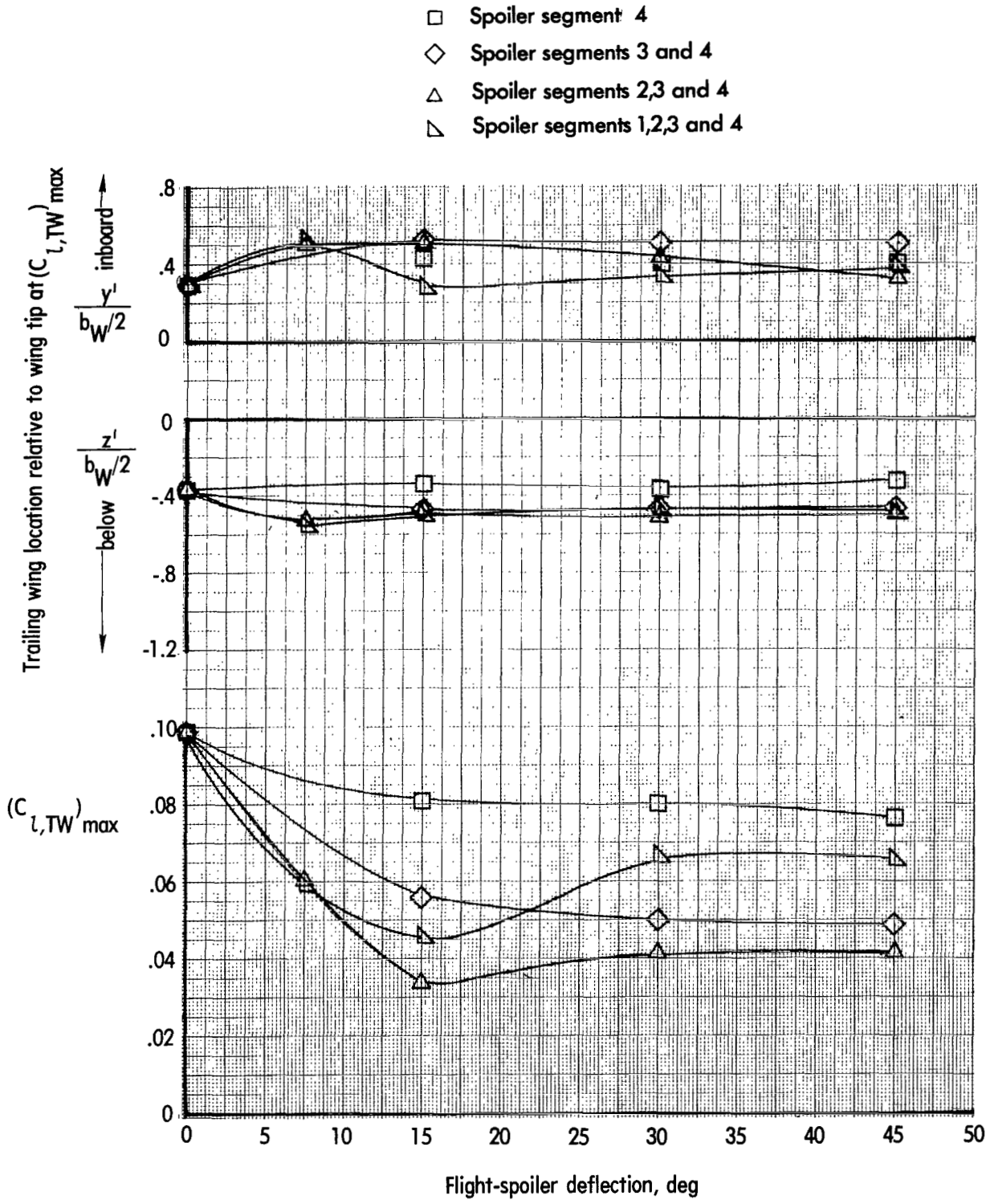

Figure 19.- Variation of trailing wing location and rolling-moment coefficient with flight-spoiler deflection for flight-spoiler segments 4; 3 and 4; 2, 3, and 4; 1, 2, 3, and 4. Trailing wing model located 7.8 transport wing spans behind transport aircraft model; $C_{L,trim} = 1.2$.

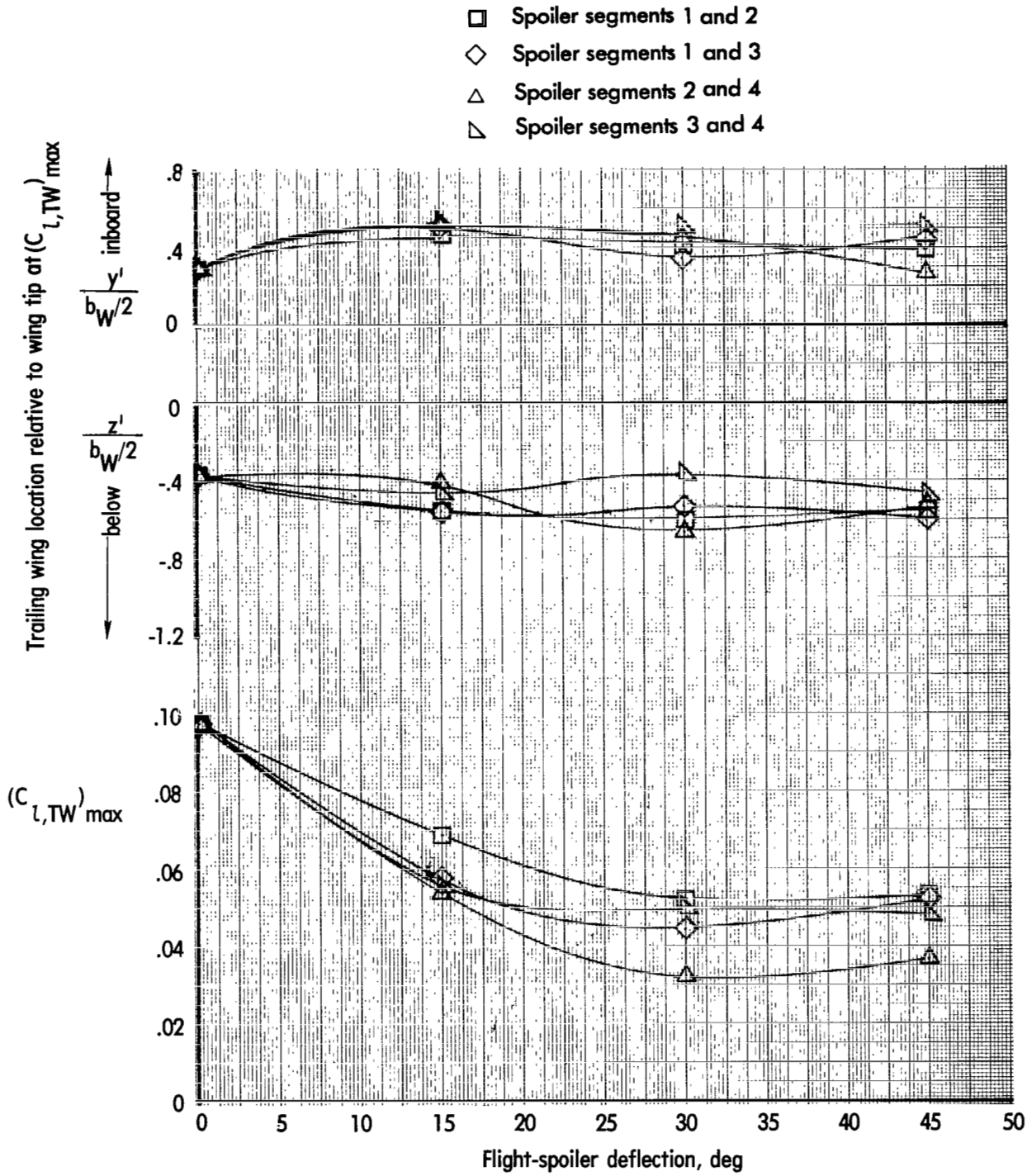

Figure 20.- Variation of trailing wing location and rolling-moment coefficient with flight-spoiler deflection for flight-spoiler segments 1 and 2; 1 and 3; 2 and 4; 3 and 4. Trailing wing model located 7.8 transport wing spans behind transport aircraft model; $C_{L,trim} = 1.2$.

1. Report No.	2. Government Accession No.	3. Recipient's Catalog No.
NASA TP-1419		

4. Title and Subtitle	5. Report Date
LOW-SPEED WIND-TUNNEL PARAMETRIC INVESTIGATION OF FLIGHT SPOILERS AS TRAILING-VORTEX-ALLEVIATION DEVICES ON A TRANSPORT AIRCRAFT MODEL	April 1979
	6. Performing Organization Code

7. Author(s)	8. Performing Organization Report No.
Delwin R. Croom	L-12622
	10. Work Unit No.

9. Performing Organization Name and Address	11. Contract or Grant No.
NASA Langley Research Center Hampton, VA 23665	514-52-03-02
	13. Type of Report and Period Covered

12. Sponsoring Agency Name and Address	14. Sponsoring Agency Code
National Aeronautics and Space Administration Washington, DC 20546	Technical Paper

15. Supplementary Notes

16. Abstract

An investigation was made in the Langley V/STOL tunnel to determine, by the trailing-wing sensor technique, the effectiveness of 11 combinations of the existing flight-spoiler segments on a jumbo-jet transport aircraft model when they were deflected as trailing-vortex-alleviation devices. All 11 of the flight-spoiler configurations investigated were effective in reducing the induced rolling moment on the trailing model. This investigation is an extension of earlier wind-tunnel and flight tests which showed that the existing flight spoilers on the jumbo-jet aircraft can be used as effective trailing-vortex-alleviation devices.

Essentially all of the reduction in induced rolling moment on the trailing-wing model was realized at a spoiler deflection of 45° for single-spoiler configurations, 30° for two-spoiler configurations, and 15° for both the three- and four-spoiler configurations.

Of the 11 flight-spoiler configurations investigated, the most promising configuration for trailing-vortex abatement on the jumbo-jet aircraft appears to be the three inboard flight spoilers deflected 15°.

17. Key Words (Suggested by Author(s))	18. Distribution Statement
Vortex alleviation Trailing-vortex hazard	Unclassified - Unlimited Subject Category 02

19. Security Classif. (of this report)	20. Security Classif. (of this page)	21. No. of Pages	22. Price*
Unclassified	Unclassified	43	$4.50

* For sale by the National Technical Information Service, Springfield, Virginia 22161

NASA-Langley, 1979

11 1 1U,A, 030979 S00903DS
DEPT OF THE AIR FORCE
AF WEAPONS LABORATORY
ATTN: TECHNICAL LIBRARY (SUL)
KIRTLAND AFB NM 87117